Synthesis and Characterization of Perylene Chromophoric Ligands for DNA Binding

Saween Nariman Mawlood Sherko

Submitted to the
Institute of Graduate Studies and Research
in partial fulfillment of the requirements for the Degree of

Master of Science
in
Chemistry

Eastern Mediterranean University
June 2014
Gazimağusa, North Cyprus

Approval of the Institute of Graduate Studies and Research

Prof. Dr. Elvan Yılmaz
Director

I certify that this thesis satisfies the requirements as a thesis for the degree of Master of Science in Chemistry.

Prof. Dr. Mustafa Halilsoy
Chair, Department of Chemistry

We certify that we have read this thesis and that in our opinion it is fully adequate in scope and quality as a thesis for the degree of Master of Science in Chemistry.

Asst. Prof. Dr. Nur P. Aydınlık
Co -Supervisor

Prof. Dr. Huriye İcil
Supervisor

Examining Committee

1. Prof. Dr. Huriye İcil
2. Asst. Prof. Dr. Hatice Nilay Hasipoğlu
3. Asst. Prof. Dr. Mustafa Erkut Özser

ABSTRACT

Perylene chromophoric derivatives are versatile compounds for many applications in various fields. Excellent optical properties such as high extinction coefficients and strong fluoresence combined with ease in electron accepting ability are the most notable advantages of perylene diimides.

This project is focused on the synthesis of different kinds of perylene dyes. A Perylene-3,4,9,10-tetracarboxylic acid monoanhydride monopotassium carboxylate (K-Salt), N-(4-hydroxyphenyl)-3,4,9,10-perylenetetracarboxylic acid-3,4-anhydride-9,10-imide (OHPMI) and N-(4-hydroxyphenyl)-perylene-3,4-dicarboximide-9,10-di (isopropyloxycarbonyl) (OHPMI-DIESTER) are synthesized. The final perylene derivative (OHPMI-DIESTER) was synthesized by consecutive reactions. OHPMI-DıESTER was especially designed to bind with DNA.

The synthesized perylene derivatives are characterized by FTIR. Their optical properties are investigated by UV-Vis and emission techniques.

Keywords: K-Salt, perylene monoimide, OHPMI-Diester, extinction coefficient.

ÖZ

Kromoforik perilen türevleri pek çok uygulama için çok yönlü birleşiklerdir. Kolay electron kabul yeteneği kolaylığı, yüksek soğurma katsayısı ve güçlü fluoresans gibi özelliklerinin birleşmesi perilen türevlerinin en önemli avantajlarındandır.

Bu projede farklı tür perilen boyaların sentezi üzerine odaklanılmıştır. Perylene-3,4,9,10-tetrakarboksilik asit monoanhidrit monopotasyum karboksilat (K-tuzu), N-(4-hidroksifenil)-3,4,9,10-perilentetrakarboksilik asit-3,4-anhidrit-9,10-imid (OHPMI), ve N-(4-hidroksifenil)-perilen-3,4-dikarboksimid-9,10-di (izopropiloksikarbonil) (OHPMI-DIESTER) sentezlenmiştir. Son perilen türevi (OHPMI-DIESTER) ardışık tepkimeler ile sentezlendi. OHPMI-DIESTER'in özellikle DNA'ya bağlanabilmesi için tasarlanmıştır.

Sentezlenen perilen türevleri FTIR ile karakterize edilmiştir. Optik özellikleri UV-Vis ve emisyon teknikler ile incelenmiştir.

Anahtar Kelimeler: K-Tuzu, perilen monoimid, OHPMI-Diester, soğurma katsayısı.

To my family

ACKNOWLEDGMENT

I would like to take this oppurtinity to extremly express my sincere appreciation and indebt edness to my supervisor Prof. Dr. Huriye Icil for allowing me to work in her group and for giving me to opportunity and resources to work on this interesting topic. I also wish to point out her great knowledge and experince not only in organic chemistry but also in general life. Her ability for teaching, telling motivating stories and of great sense to give rise of someones interest in chemistry, particulary organic chemistry aspect. With her invaluable supervision, all my efforts could have been short-sighted.

My great appreciation go to my co-supervisor Asst. Prof. Dr. Nur Paşaoğullari Aydınlık for her patience and advice. They always encouraged me to pass through the hard time in conducting this research.

I would like to express my sincere gratitude to Dr. Dugu uzun for her immense knowledge; her guidance helped me in all stages of the research and thesis writing.

Iam also greatfull to everyone in the organic group for thier assistance and friendship.

Finally, I woul like to express my gratitude for my parents, brothers, sisters, my father in law, my mother in law and my husband (Dawan) for thier continous support and encouragement and I would like to extend my thanks to all who helped me during this study.

TABLE OF CONTENTS

LIST OF TABLES

LIST OF FIGURES

LIST OF ILLUSTRATIONS

LIST OF SYMBOLS/ABBREVIATIONS

Å	Armstrong
Cm	Centimeter
^{0}C	Degrees celcius
$\Delta\bar{\nu}_{1/2}$	Half-width of the selected absorption
ε_{max}	Maximum extinction coefficient
E_s	Singlet energy
F	Oscillator strength
λ_{exc}	Excitation wavelength
λ_{max}	Absorption wavelength maximum
τ_0	Theoretical radiative lifetime
τ_f	Fluorescence lifetime
Φ_f	Fluorescence quantum yield
Nm	Nanometer
$CDCl_3$	Deutero-Chloroform
CH_2Cl_2	Dichloromethane
$CHCl_3$	Chloroform
CHL	Chloroform
CV	Cyclic Voltammetry
DMF	N,N'-dimethylformamide
DMSO	N,N'-dimethyl sulfoxide
DNA	Deoxyribonucleic acid
DSC	Differential Scanning Calorimetry
FT-IR	Fourier Transform Infrared Spectroscopy

HCl	Hydrochloric acid
KBr	Potassium bromide
K_d	Rate constant of Radiationless deactivation
K_f	Theoretical fluorescence rate constant
KOH	Potassium hydroxide
M	molar concentration
MeOH	Methanol
NaOH	Sodium hydroxide
NMR	Nuclear Magnetic Resonance Spectroscopy
RNA	Ribonucleic acid
UV-vis	Ultraviolet visible absorption spectroscopy

Chapter 1

INTRODUCTION

Perylene dyes (Perylene-3,4:9,10-tetracarboxylic bisimides, PDIs) chemistry was detected in 1913 and these dyes are important pigments and are of particular importance due to the high fluorescence quantum yields ($\Phi_f \approx 1$) in organic solvents, they have large molar absorption coefficients (ε_{max}), high thermal, chemical and photo stabilities under visible light irradiation and ease of tunable absorption properties [1-6].

PDIs are inexpensive and they are readily available compounds. Moreover, they display singlet energy transport over long distances and because of their unique photophysical and optical properties they have attracted great interest. The application areas for PDIs are light-harvesting equipments, organic field-effect transistors and solar cells. Their solubility is significant in assessment to their use implementations with high efficiency [7].

Perylene dyes have a number of attributes that make them convenient for inclusion into covers containing high tinctorial strength, high thermal constancy, good condition stability and good photo stability [8].

In general development and the investigation of new symmetrical and antisymmetrical PDIs are significant to understand sensitizing materials [9].

PDIs are mostly used photovoltaic applications as a n-type semiconductor system, in optical and electrical applications, such as dye lasers technology, field effect transistors, electro photographic devices, photorefractive thin film technology and organic light-emitting diodes.

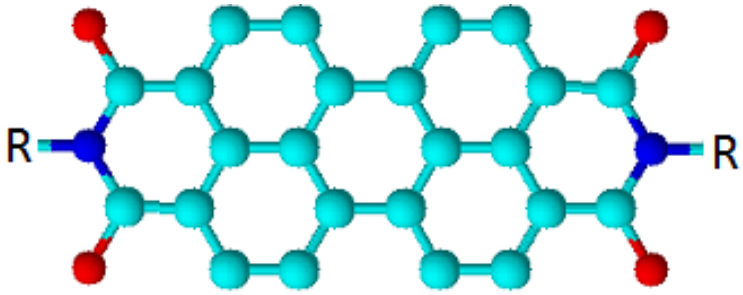

Figure 1.1: Common Structure of Perylene Diimide (PDI)

Perylene-3,4:9,10-tetracarboxylic bisimides (PDIs) shown in Figure 1.1 and perylene monoimides (PMIs) shown in Figure 1.2 present an important benefit in biological areas as well as electronic areas [10].

Perylene monoimides have been a benefit median for designing of unsymmetrical perylene dyes. Due to their low yield the synthesis methods of PMI dyes have been developed rapidly over the past year [11].

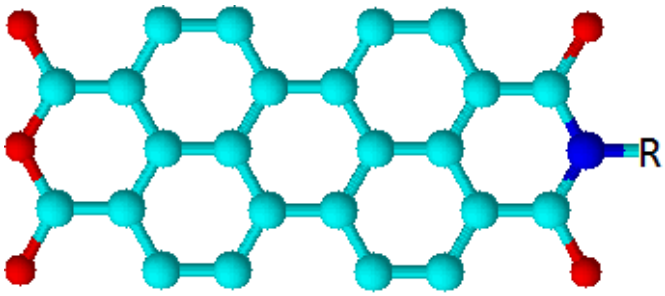

Figure 1.2: General Structure of Perylene Monoimide (PMI)

PMIs with attached solubilizing aryloxy substituents on the N-arylgroup are valued structure blocks for integration as extention dye in porphyrin-based light-harvesting matrices [12].

A method for diverting the commercially available PDA to PMI which supply the starting point in most way to replaced PMI pigments is by Langhals [13]. Methods for halogenation and replacement of perylene-monoimide dyes has included perylene-monoimide dyes in dendrimeric buildings has progressed by Müllen [14-16]. A type of PMI dye for employing in molecular photonic switches has developed by Wasielewski [17-21].

On the other hand, Deoxyribo Nucleic Acid (DNA) as shown in Figure 1.3 is the genetic material which moves in all living organisms. DNA is made up of two anti-6 parallel strands composing nucleotides which are the basic construction blocks of DNA. In addition, any nucleotide contains some structures like phosphate, sugar and one organic base such as Thymine (T), Cytosine (C), Guanine (G) and Adenine (A). Thymine and Cytosine are classified as pyrimidin bases. Guanine and Adenine are classified as a purine bases. Pyrimidine is a class of single-ringed organic bases. Purine means a class of double- ringed organic based found in nucleic acids [22].

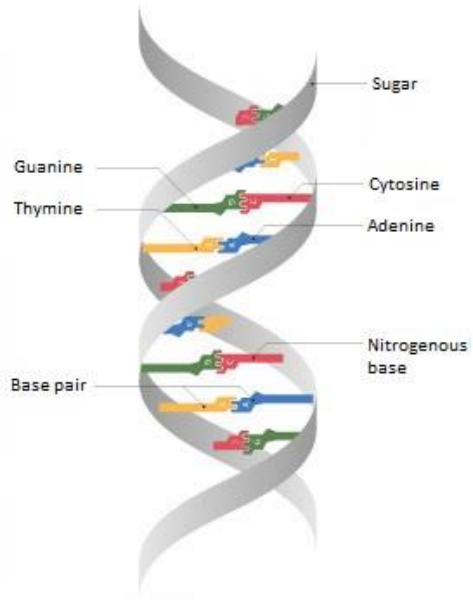

Figure 1.3: Structure of Deoxyribo Nucleic Acid (DNA)

The interaction between nucleic acids with small molecules such as organic dyes and drugs, has been studied intensively as it provides knowledge on the screening and design of novel and more effective drugs targeting DNA and can possibility accelerate the development processes and drug discovery. The interaction of anti-carcinogenic medicines with DNA has been studied and they are significant to improve new cancer therapy remedies [23].

DNA for nonbiological applications has aroused much interest in recent years. The controllable diverse structures and robust physicochemical nature of G-quadruplex DNA make it a promising candidate as catalyst, biosensor, nanomachine and the construction of functional DNA nanostructure [24].

Recently many G-quadruplex-binding small molecules have been developed, most of which are nitrogen-containing compounds. Because electrostatic interactions strongly participate in ligand–quadruplex binding, the introduction of a steady positive charge via alkylation of the nitrogen atom of these compounds has been put forth as one potential idea for improving their quadruplex binding and stabilization abilities [25].

Perylenediimide derivatives and several types of other molecules like isoquinoline alkaloids, indolealkaloids, pyrrolimidazol polyamides, synthetic indole derivatives that interact inside DNA as shown in Figure 1.4 [23].

Increasing their binding properties by coupling to other compulsory types like nucleic acids is possible. For the discovery of specific genes the easy decline of these compounds has let them to be applied as electrochemical DNA biosensors [26].

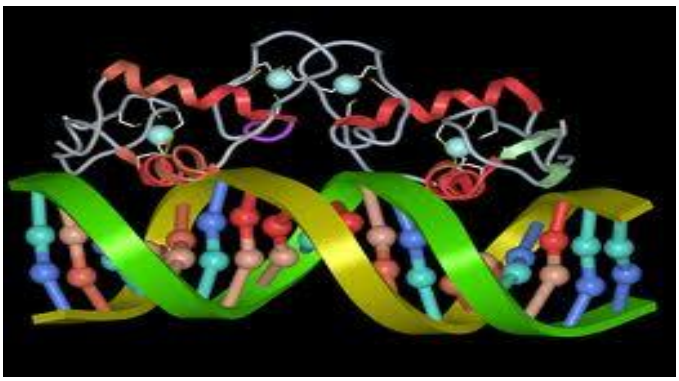

Figure 1.4: Deoxyribonucleic Acid (DNA) Binding with Different Molecules

The objective of this work is to synthesize various perylene derivatives toward efficient perylene ligands with quaternized amine groups. Perylene chromophoric ligands can be prepared via three steps, where the final compound can bind to DNA and the representative diagram is shown in Scheme 1.

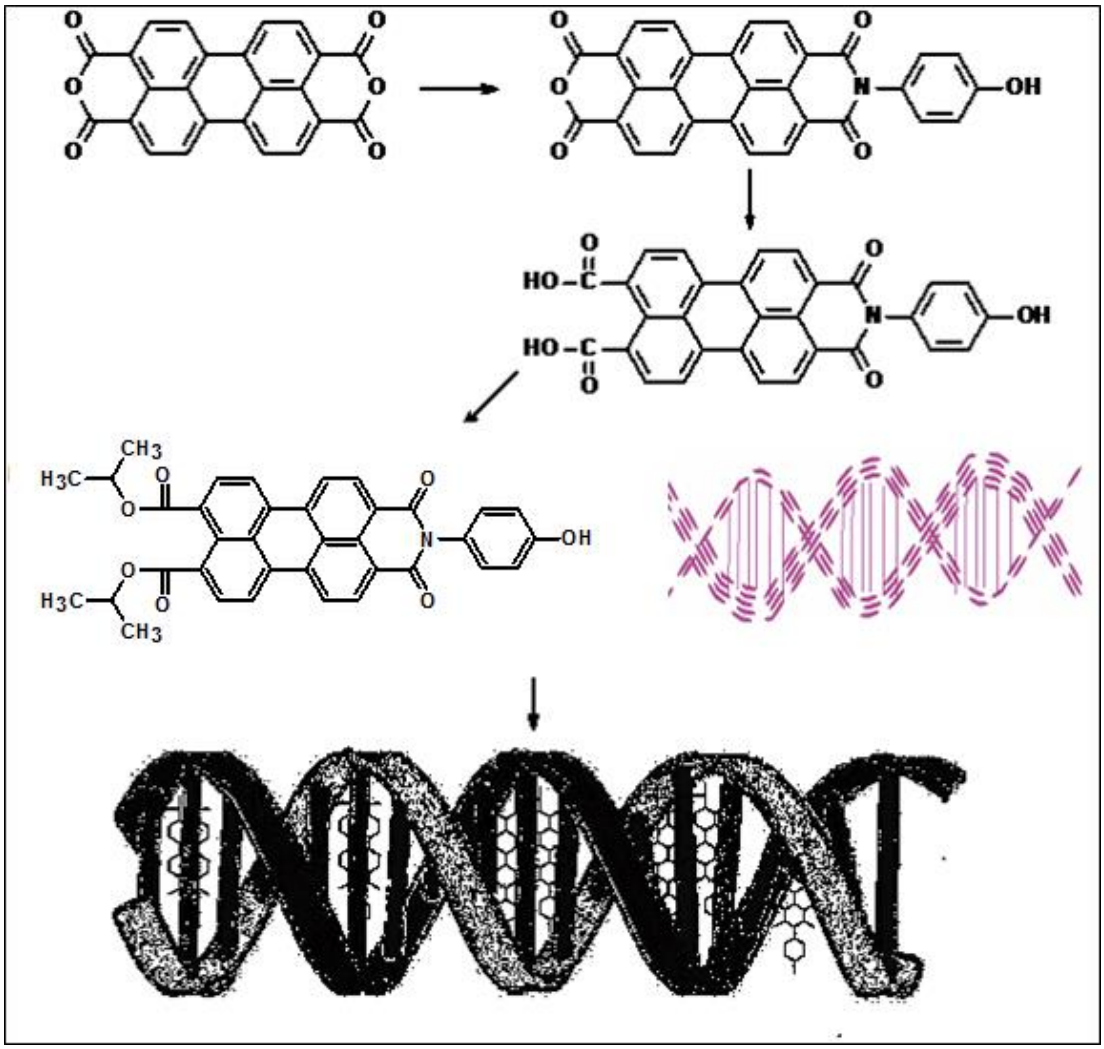

Scheme 1.1: Synthesis of Various Perylene Derivatives and Representative DNA Binding to Perylene Derivatives.

The synthesis includes synthesis of a perylenemonoimide followed by carboxylic acid monoimide and its OHPMI-Diester. Later, the compounds will be investigated to explore their potential using UV-vis and emission techniques. Structural characterization will be performed by FTIR.

Chapter 2

THEORETICAL

2.1 Structural Aspects of DNA

DNA structure was unknown until 1953 when Watson and Crick determined it through X-ray crystallography which is obtained by Rosalind Franklin. They described the DNA as a double helix that adopts different three-dimensional conformations although the most common form of the double stranded DNA is the "B" form, characterized by a "right-handed" helix. As it is shown in Figure 2.1 the backbone of the DNA strand is consisted of alternating phosphate and sugar groups with the base linked to each sugar as side chain pair held by hydrogen bonds between particular pairs of bases. The precise base pairing in their DNA helix model suggested an obvious copying mechanism for genetic material. Therefore, DNA has been identified as a primary target for anticancer drugs which can change DNA conformation and inhibit duplication or transcription and is considered one of the most promising biological receptors for the development of chemotherapeutic agents [27].

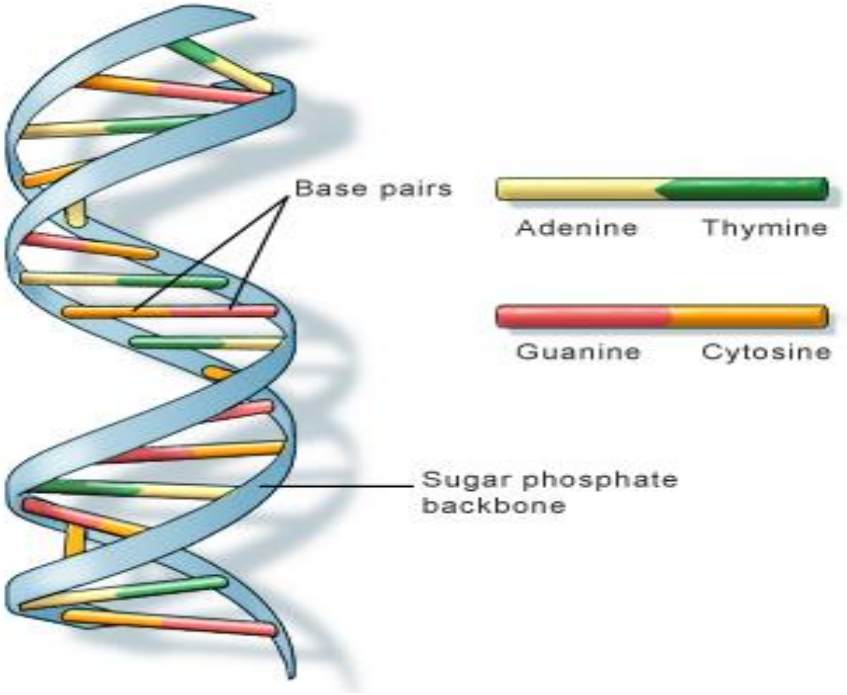

Figure 2.1: Structure of DNA

2.1.1 Theoretical Aspects of G-Quadruplex Nucleic Acid Sequences

The idea that nucleic acids rich in guanine are self-associated has a long historyas compared to the double helical structure discovered fifty years ago. Gel formation in those days was less of scientific values and created much confusion in the minds of researchers based on its sequential method of formation. Figure 2.2 shows a model of Hoogsteen bonded hydrogen bonded-guanine tetrad or G-quartet which is a basic keynote for organization. This model or concept was obtained due to an association at the basis of the molecule which resulted from its physical studies and diffraction of its fiber.

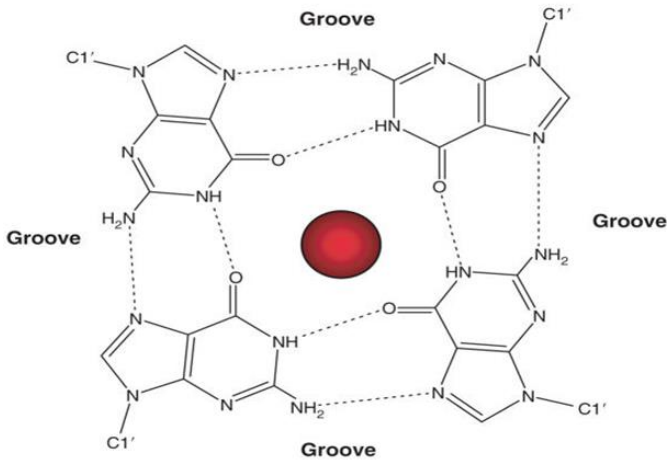

…….**:** Hydrogen Bridge

Figure 2.2: Design of G-bases in a guanine quartet with a metal ion at its core.

Quadruplexes can be composed from one, two or four detached branches of DNA or RNA and can view a large range of topologies which are in part a result of different potential groups of branch trend as well as differences in episode size and series. They can be defined in general terms as structures consists of a core group of at least two stacked G-tetrads, which are held together by episodes emerging from the interference mixed-sequence nucleotides that are not usually participate in the tetrads themselves. The combination of the number of stacked G-tetrads, the polarity of the branches and

the sites and length of the episods would be expected to lead to a plurality of G-quadruplex built, as indeed it is found experimentally.

G-quadruplexes are higher-order RNA and DNA structures composed from G-rich chains that are built around tetrads of hydrogen-bonded guanine bases. Potential quadruplex chains have been identified in G-rich eukaryotic telomeres and more recently in non-telomeric genomic DNA, e.g. in nuclease-hypersensitive promoter areas. The natural role and biological validation of these structures is starting to be discovered and there is special attention in them as goals for therapeutic interference [28].

2.2 Potential π-Conjugated Molecules for DNA Sequence Binding

Derivatives of perylene diimide (PDI) and Naphthalene diimide (NDI) can intervene in DNA cores [26].

The general structure of PDI is given in Figure 2.3 which are one of key ligands in photodynamic treatment coupled with G-quadruplex DNA stabilization and inhibition of telomerase activity in cells cancer [10].

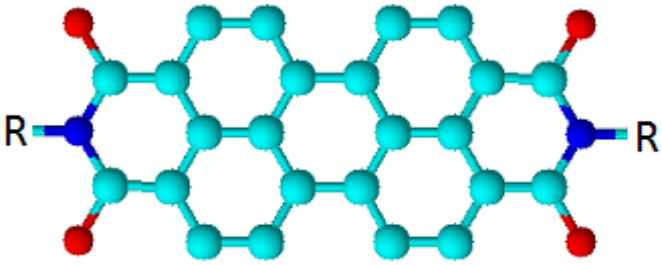

Figure 2.3: General Structure of PDI

Perylene diimide can be made to reach accepted solubility equilibrium and possibilities of arranging stacks on broader overlapping of p-intermolecular orbital by alternations on the π-π face – to – face interactions which in domains of photonics are essential for visualized applications [26].

In photodynamic treatments, perylene dyes produce active oxygen types, which initiate the oxidation of cancer cells under visible light rays. There has been currently great importance in exploring the possibility of G-quadruplex DNA binding selectivity of PDI dyes. This selectivity has crucial stage of inhibition of human telomerase, which is responsible for increase of cancer cells [10].

It is shown in Figure 2.4 that thread intercalation models are used as synthetic path

ways for PDI novel derivatives used for DNA duplex attachments [29].

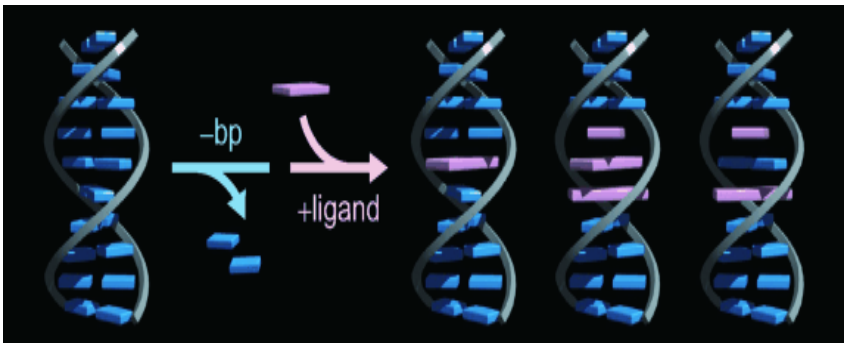

Figure 2.4: How PDI binds to DNA

Between aromatic molecules that have found interest, the naphthalene diimides (NDIs) where the general structure given in Figure 2.5 have attracted much interest because of their tendency to form n-type over p-type semiconductor materials. The naphthalene diimides (NDIs) are a compact, electron incomplete class of aromatic compound able to self-organisation and being incorporated into larger multicomponent councils through intercalation [30].

The thermal stabilities, solution processability and efficient electron accepting characteristics of Naphthalene diimide NDI has pull a major concern in the world of today. Materials made up of NDI are widely employed in molecular switches, sensors, and supramolecular assembly [31].

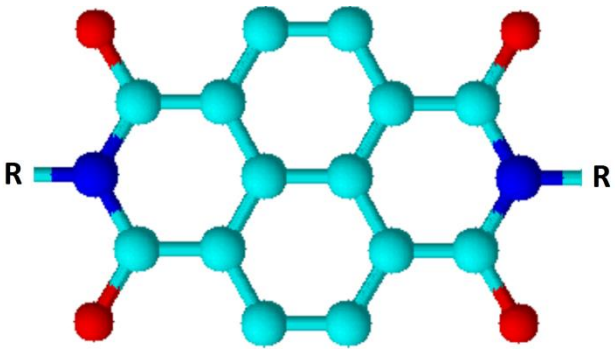

Figure 2.5: General structure of NDI

It is shown in Figure 2.6 that thread intercalation models are used as synthetic path ways for NDI novel derivatives used for DNA duplex attachments. In such a model, insertion of NDI into a DNA molecule is done such that chains made up of two sides pushed to rest in opposite DNA grooves.

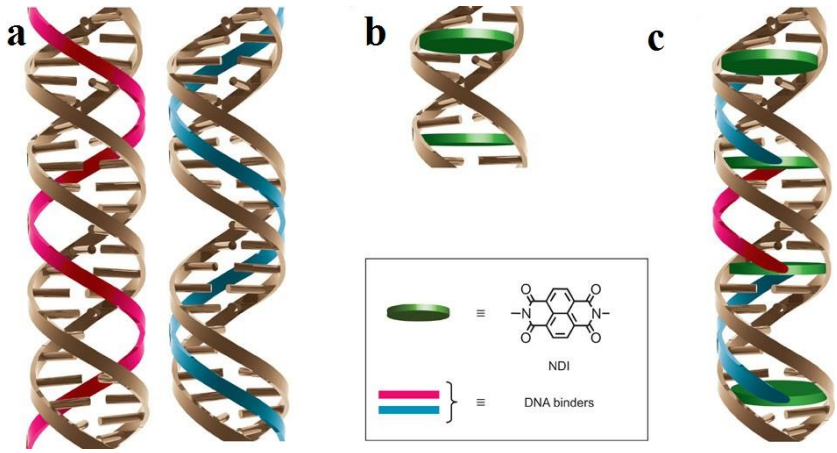

Figure 2.6: How NDI binds to DNA

a-DNA-binding molecules designed to form a triple helix with DNA strands in either the major (left; pink) or the minor (right; blue) groove.

b-Intercalation of naphthalene diimide units (NDI, green) between base pairs. The peptide linkers are omitted for clarity.

c-Model of the highly stable tetra-intercalator complex formed by four NDI units linked through three groove-binding peptide linkers that bind to the double helix in a minor grove–major grove–minor grove combination.

Threading intercalators which serves as drug carriers in its designing possess some advantages such as creating additional patterns of recognition within the setup by coordinating substituents into opposite DNA grooves. This creates selective possibilities for changing substituents in medicinal agent developments as well as big probes of DNA dynamics with large amplitudes [29].

As it is shown in Figure 2.7, polyamides composed of Pyrrole and Imidazole are small particles that bind with specified sequencing to DNA molecules and are used as modules for DNA binding. Polyamides of Py and Im can be used to identify specific sequences of DNA in a minor groove of DNA. In Im possesses lone pair of electrons creates hydrogen bonding between the 2-amino hydrogen found in the guanine. Im/Py pairing is antiparallel and denotes Guanine – Cytosine while that of Py/Im denotes cytosine – guanine. Also Py/Py anti parallel pairing deteriorates Thymine – Adenine or Adenine – Thymine linkages. Polyamides of Py-Im can linked to specified sequences of DNA as compared to binding DNA proteins, it is logical to produce polyamides of Py-Im with distinctive richness in guanine-cytosine promoting sections which controls expression of genes. Very rare recognition sequencing of polyamides of Py-Im is 50-CGCG-30 and 50-GCGC-30 with higher acknowledgement due to their high planarity polyamides Im [32].

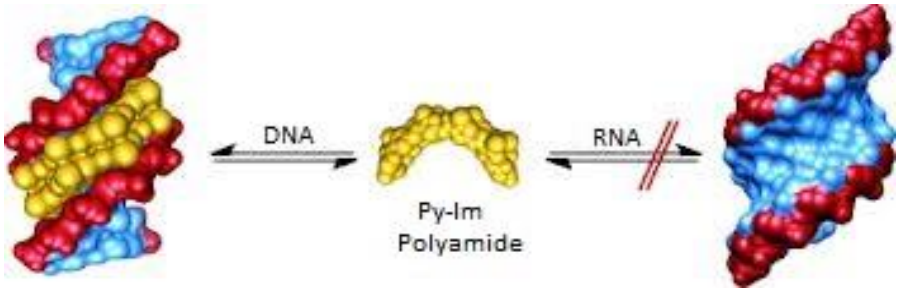

Figure 2.7: Pyrrole imidazole with DNA

Genomic utilizations of DNA-binding molecules need an unbiased knowledge of their high affinity sites the high-throughput analysis of pyrrole-imidazole polyamide DNA-binding specificity in a 1012-member DNA chain library using affinity purification coupled with massively parallel sequencing [33].

2.2.1 G-Quadruplex-Interactive Ligands

Smaller molecules bonded non-covalently to nucleic acids serves as essential categories for antibacterial, antitumor and anticancer therapies [34].

Linear chromosomes are protected at their ends by specialized deoxyribonucleic acids sequences called telomeres and are found in humans as repetitive and highly preserved cycles of hexa nucleotides (TTAGGG) and are of 5-10 kb in length. The guanine rich telomeric repetitions can combine to produce guanine quadruplex deoxyribonucleic acids secondary structures known as G4's. This comprises of guanine tetrads planes linked together and balanced by monovalent cations for example K^+ and Na^+ bridged together by a network Koogsten hydrogen bonding.

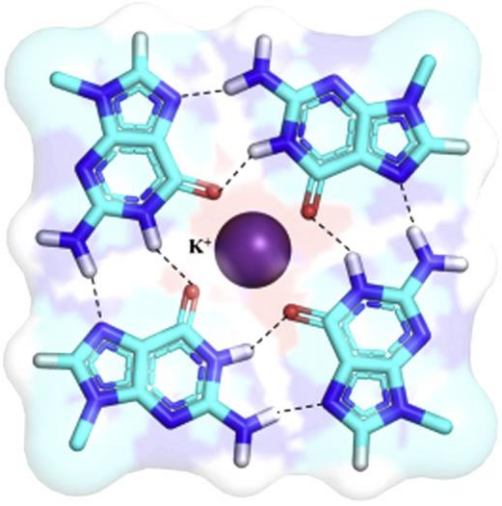

Figure 2.8: Guanine bases including the central potassium cation

Figure(2.8) shows quinine quartet representing network of H-bonding existing in the Hoogsteen and Watsone Crick guanine base 'faces' with potassium cation at the center of the quadruplex design to stabilized it. Even though the telomeric sequence found in humans are regarded to be a simple G4, we can have it folded in up to two hundred intramolecular forms having different connecting loop types (i.e. double

reversal chains, diagonal, and lateral), segmented orientated strands, antiparallel and parallel, guanine quartets numbers i.e. three or two, and torsion glycosyl angles *i.e.* anti or syn relying on the situations. Depending on categories of cations, several reports have been allocated for sequencing of DNA possessing d(TTAGGG) units with different unimolecular guanine quadruplexes. Wang & Patel (1993) discovered the first topology applying NMR spectroscopy in a solvent of Na^+. It was found to fold as anti-parallel guanine quadruplex made up of three stacked guanine quartets having 2 diagonal and lateral loops of connection. Parkinson et al (2002) used Crystallographic X ray to demonstrate that in K^+, telomeric sequencing found in humans shown as parallel topology with 3 stacks of quartets of guanine and reversible double chain loops [35].

2.3 Structural Aspects of Perylene Chromophoric Dyes

Resonance energies in carboxylic imides are very high and even more than that witnessed amides of carboxylic acids which renders them stable. Addition of 5(1) or 6(2) heterocyclic ring member gives them enhanced stabilization.

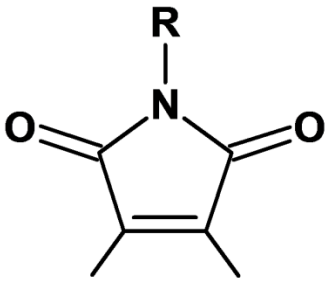

Figure 2.9

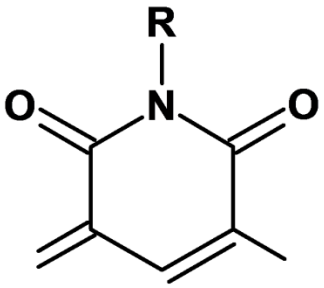

Figure 2.10

Figures 2.9 and Figure 2.10 are important as parts of the design of certain compounds which demands for higher persistency. When the element in Figure 2.10 is fixed to the peri-position of perylene it produces a perylene dye belonging to the tetracarboxylic bisimide family.

Perylene dyes were discovered in the 1913 by Kardos and they were found to be dyes with high light fast. They were also used as technical pigment as a result of their low solubilities. Their excellent fluorescent potential was not known before 1959 making them not to obtain a wide range of applications. Their unique characteristics and substantial fluorescence of the perylene dyes increased their novel uses [1].

Also PDIs made up of perylene containing imidic materials. Potential uses in electronics of molecular organics. Applied as electrochromic and light emitting substances. They have high fluorescence quantum yields of $\varphi_f \cong 1$ witnessed in

fluorescence and has an efficient absorption in the visible region of the spectrum with higher coefficients of molar absorption (ε_{max}). The huge fluorescence capacities of perylene dyes allocate fluorescent labeling characteristics on them.

PDIs are thermally stable substances. Like perylene, the derived PDI are classes semi-conductors which are n-type. These dyes are used in: organic electronic systems, light-harvesting systems, transistors and devices of PVs nanoelectronic devices. They provide tailoring at imide positions of side chains with multiple medieties. PDIs are used in DNA binding as chromophoric dyes. The generation of diverse conjugate with multiple medieties that bind simultaneously via DNA grooves recognitions offers interactions which are non-covalent stacking, thus going to ligands with efficient specificities and affinities [36].

2.3.1 Functional Properties of Perylene Derivatives

The derivatives of perylene dyes have a high reflectance in the NIR region and as a result are used in camouflage paints. Dyes based on perylene coupled with its ability to absorb in the NIR region have all the properties of colourants with high performances including high photo, weather and thermal stability with acceptable painting strengths. Apart from pigments, compounds of pereylene are widely used to make devices of optoelectronics photonics, emitting light diodes, field effect transitors, solar cells and photoreceptors for electro-photography [37].

Antisymmetric and symmetric derivatives of PDIs have found wider applications in producing OLED, LCD, photodynamic therapies, OFED, dye lasers, chemical oxidation photosensitizers, dye synthesized solar cells (DSSCS) and stabilization of deoxyribonucleic acids guanine (DNA) quadruplexes [38].

Also, due to their pi-electron conjugation, derivatives of PDI attracted a lot of attention as organic electronics substances. In the case of its usage for electronic applications, a vital issue was the solubility of the chromophores and to counter this several strategies on the addition of chemical groups to improve its solubility was proposed by adding these groups to several sites on the structure of perylene. Nowadays, derivatives of PDIs are one of the most studied molecular systems and because of its unique combination of physical characteristics have found several applications in almost every part of organic optoelectronics. In electrophotography and photovoltaics derivatives of perylene dyes are widely used because of their high thermal stability, optical and redox properties. In recent times thin-film transistor that are stable in air have been produced. Fixed molecular designs of cores of PDI results in an elevated fluorescent quantum yield thereby creating attractive derivatives of PDI

for laser dyes for example, most popular red and orange perylene dyes, fluorescence labels and collectors of light, emitters in OLED and fluorescence sensors. Derivatives of PDI substituted by imide nitrogen shows a predominant photo and thermal stabilities which demonstrates fluorescence quantum yield closed to a hundred percent and possess small spectral handleabilities. Promising derivatives of perylene are those with substituting couplings at their bay positions Figure 2.11 due to the prevention of lower luminescent quenching by the introduction of core perylene twisting and steric hindrance by the substituent at the bay position [39].

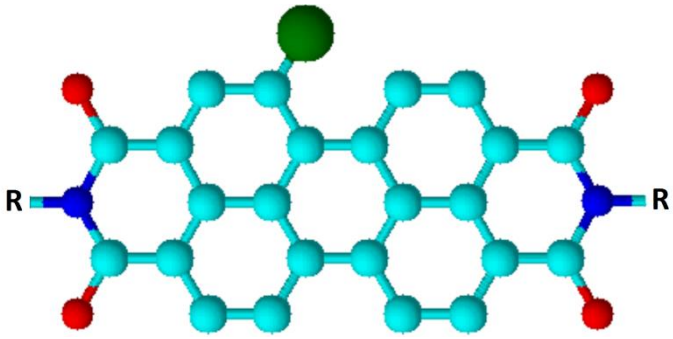

Figure 2.11: PDI substituted at Bay Position

Derivatives of perylene possesses liquid crystallized characteristics which are brought about by parallel stacking of p-p* between cores of neighboring perylene. Derivatives of perylene which have been modified larger substituent shows liquid crystalline, semi-conducting and excellent processability characteristics which can be applied widely in future usages. Privacy Technical Assistance Center materials possessing alkyl substituent linked to the core of the perylene leads to improved solubilities of derivatives of perylene largely in solutions. This characteristic of improving properties can be assigned to the long chain present with decreased intensity of charges on packaged terminal air conditioner [40].

2.3.2 Structural Analysis of G-Quadruplex/Perylene Dye Ligand Interactions

Guanosine-rich DNA chains can built constant secondary structures known as G-quadruplexes, the building blocks of which are tetrads made of four hydrogen bonded guanine bases (G-tetrads). There is a great importance in understanding the dynamic nature and potential biological roles of G-quadruplex structures. Evidence that these structures have biological roles also comes from the identification of enzymes that recognize and process G-quadruplexes including nucleases that cleave G-quadruplex DNA. Recent proposals for the role of G-quadruplex structures as 'sinks' for oxidative DNA damage has led to an increased importance in studies of the possibility roles of G-quadruplex structures in oxidative telomere shortening and division [41].

An important strategy to overcome growing problems of undesirable accumulation of dyes in tumors in PDT applications is the drug delivery to the target tumors which is called as targeted photodynamic therapy. To avoid the aggregation of the photosensitizers in healthy tissues, new strategies have been developed to rise the specific aggregation of the photosensitizers at the target site of the tumors. One of the strategies of targeting photosensitizers to the tumor cells is the use of small molecules binding to G-quadruplex, a sort of square where the last few guanosine at the end of each telomere can fold into. The nature of G-quadruplex structures suggests that they can operate as new therapeutic targets using designed small molecules to stabilize these special G-quadruplex structures [42].

2.3.3 Design of Perylene Dye Ligands for Selective Binding

G-Quadruplex structures are unique structures which could adopt from telomeric DNAs under physiological condition. G-Quadruplex structures are usually formed by stacking G-quartets. It is well known that G-quadruplexes have the ability to inhibit the telomerase activity efficiently and become potential therapeutic agents. A big number of small molecule ligands (G-quadruplex binders) that facilitate G-quadruplex formation and consequent G-quadruplex DNA structure stabilization were widely studied as they inhibit telomerase activity and are therefore used as potential drugs.

The ligands that were bound to G-quadruplexes have been suggested to end stack or form interactions in the episodes. The molecules which can selectively recognize G-quadruplex grooves are much more limited. In addition, conjugated molecules have the advantage to provide thermodynamic stabilization, induction of fluorescence and electron transfer properties.

PDI also shows an essential role in telomerase activity inhibition in cancer cells and stabilization of guanine quadruplex deoxyribonucleic acids. PDI serves as production houses for active species of oxygen during photo-dynamic therapies which initiates cancer cell oxidations under irradiation of visible light. Dyes of PDI and guanine quadruplex DNA selective attachments have remain a prime interest for most scientists. This aspect of selectivity plays an important role in inhibiting telomerase enzyme in humans thereby preventing the development of cancer cells. A huge amount of derivatives of PDI which are soluble in water containing unlike side chains are being synthesized and analyzed as cooperating ligands to guanine quadruplex designs [10].

Chapter 3

EXPERIMENTAL

3.1 Materials

Perylene-3,4,10-tetracarboxylic dianhydride, potassium hydroxide, isopropanol, chloroform, ammonium chloride, sodium sulfate, hydrochloric acid, potassium carbonate, 4-aminophenol were obtained from Aldrich. There was no more purification for all the chemicals purchased. The common organic solvents were of crude quality and were distilled according with the standard literature procedure. Distilled methanol, dimethyl form amide (DMF) and chloroform are used for solubility tests.

3.2 Instrumentation

Infrared Spectra

Infrared spectra were acquired through KBr pellets by using JASCOFT-IR-6200 Spectrophotometer by using KBr pellets.

Ultraviolet (UV-vis) Absorption Spectra

The UV-vis absorption spectra were recorded by using a Varian Cary-100 spectrophotometer of compounds in different solvents.

Emission Spectra and Excitation Spectra

Varian-Cary Eclipse fluorescence spectrophotometer was used to record Emission of the synthesized compounds. For the emission spectra of all the synthesized perylene derivatives were excited at λ_{exc}= 485 nm.

3.3 Methods of Syntheses

The aimof this study is to synthesis and design new perylene derivatives toward efficient perylene ligands with quaternized amine groups. It can be prepared via three steps process where the final compound can bind to DNA and the representative diagram is shown in Scheme 3.1.

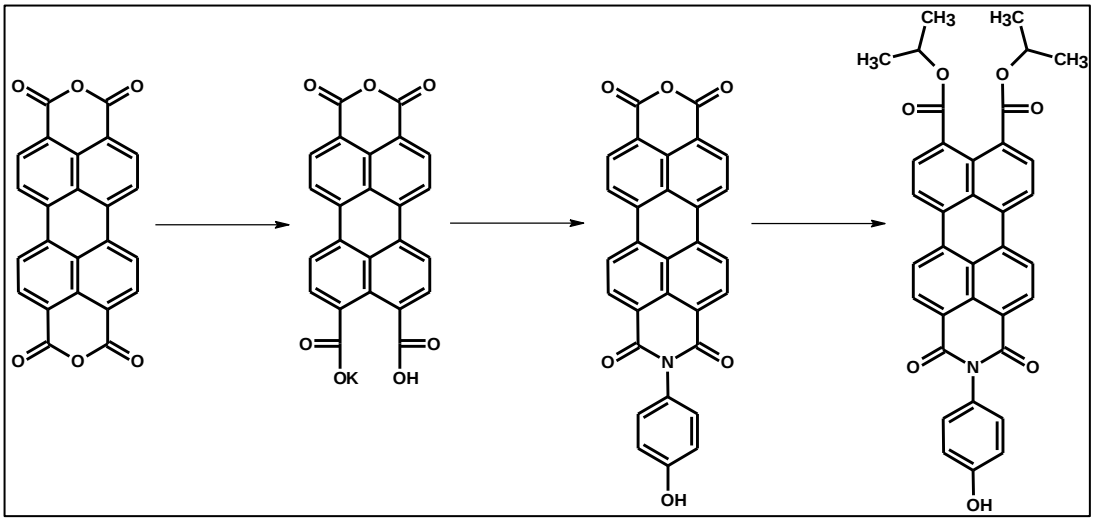

Scheme 3.1: General Reaction Scheme

According to Scheme 3.1 the starting material perylene dianhydride (PDA) was converted to Perylene-3,4,9,10-tetracarboxylic acid monoanhydride monopotassium carboxylate (K-SALT) in the first step. In the second step, Perylene-3,4,9,10-tetracarboxylic acid monoanhydride monopotassium carboxylate (K-SALT) was converted to N-(4-hydroxyphenyl)-3,4,9,10-perylenetetracarboxylic-3,4-anhydride-9,10-imide (OHPMI) and then it is converted to N-(4-hydroxyphenyl)-perylene-3,4-dicarboximide-9,10-di-(isopropyloxycarbonyl) (OHPMI-DIESTER) in the third step.

In the first step, the starting material Perylene dianhydride (PDA) was converted to a Perylene-3,4,9, 10-tetracarboxylic acid monoanhydride monopotassium carboxylate (K-SALT) in presence of KOH and phosphoric acid as it is shown in Scheme 3.2.

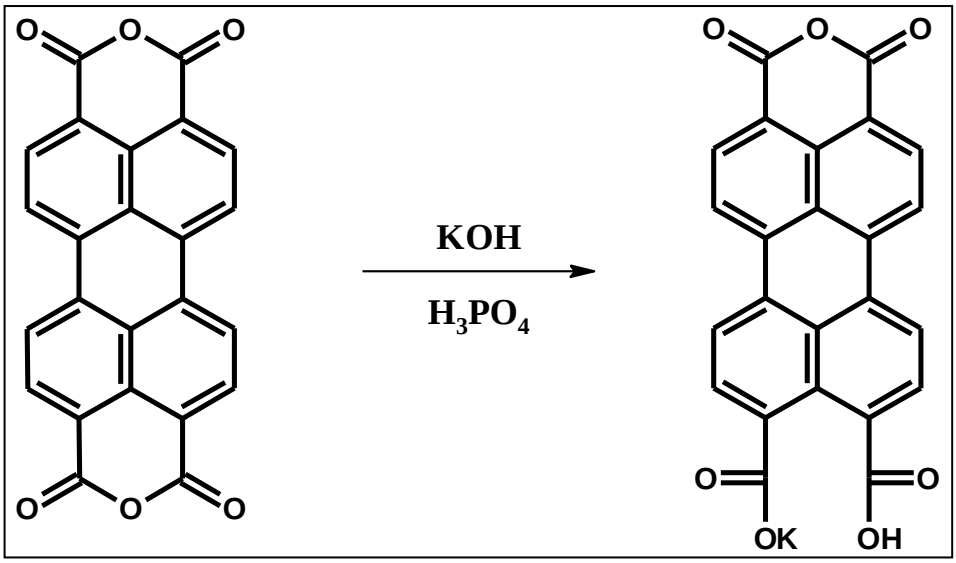

Scheme 3.2: Synthesis of Perylene-3,4,9,10-tetracarboxylic acid monoanhydride monopotassium carboxylate (K-SALT)

In the second step, the synthesized of Perylene-3,4,9,10-tetracarboxylic acid monoanhydride monopotassium carboxylate (K-SALT) was converted to N-(4-hydroxyphenyl)-3,4,9,10-perylenetetracarboxylic-3,4-anhydride-9,10-imide (OHPMI) in presence of 4-aminophenol as shown in Scheme 3.3**.**

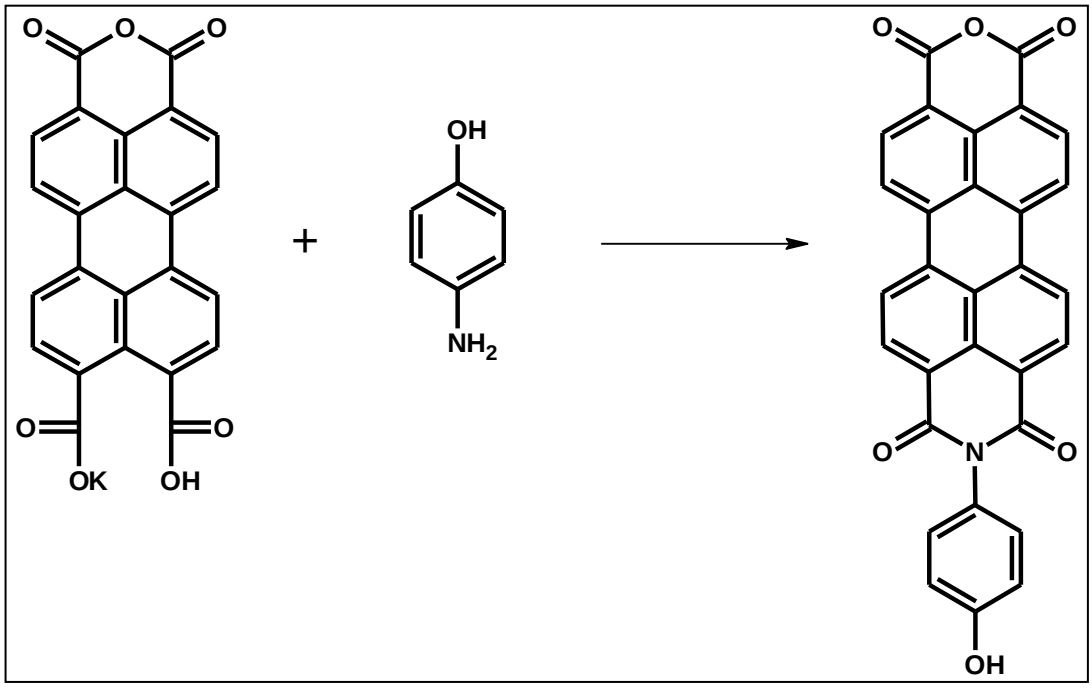

Scheme 3.3: Synthesis of N-(4-hydroxyphenyl)-3,4,9,10-perylenetetracarboxylic-3,4-anhydride-9,10-imide (OHPMI)

In third step, the synthesized of N-(4-hydroxyphenyl)-3,4,9,10-perylenetetracarboxylic-3,4-anhydride-9,10-imide (OHPMI) was converted to N-(4-hydroxyphenyl)-perylene-3,4-dicarboximide-9,10-di-(isopropyloxycarbonyl) (OHPMI-DIESTER) in the presence of isopropanol as shown in Scheme 3.4.

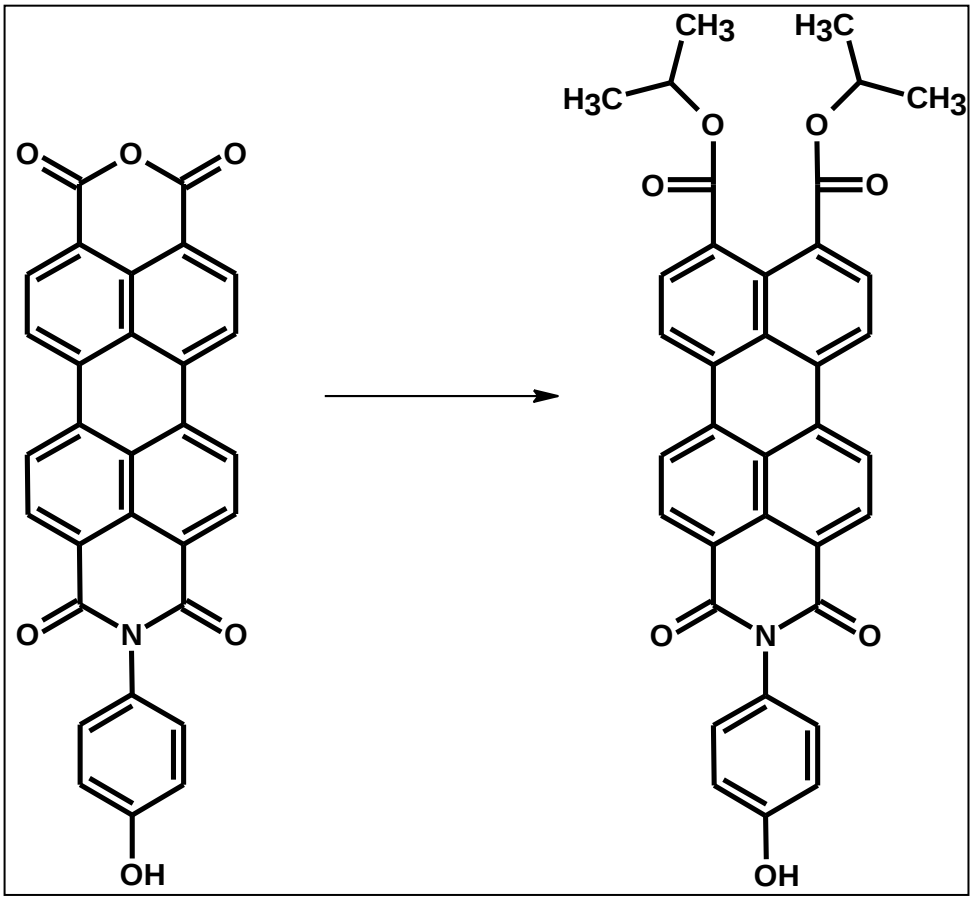

Scheme 3.4: Synthesis of N-(4-hydroxyphenyl)-perylene-3,4-dicarboximide-9,10-di-(isopropyloxycarbonyl) (OHPMI-DIESTER)

3.4 Perylene-3,4,9,10-tetracarboxylic acid monoanhydride monopotassium carboxylate (K-Salt)

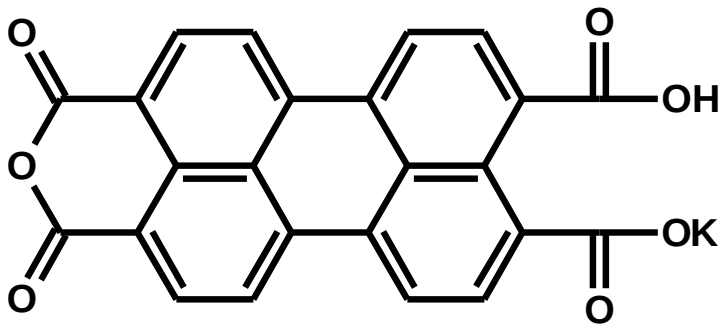

The Perylene-3,4,9,10-tetracarboxylic acid dianhydride(3g, 7.6 mmole) was stirred in KOH solution (5%, 35 ml) for 4h at 90°C. After cooling to room temperature, 12.5 ml H_3PO_4 (10%) was added and stirred for 1h at 90°C. The precipitate formed was filtered, washed with water and dried in vacuum at 100°C [9].

Yield: 89% (3.1 g, Bordeaux-red powder).

FT-IR (KBr, cm^{-1}): 3442, 3067, 1766, 1725, 1594, 1508, 1377, 1316, 1231, 1151, 1008, 945, 854, 809, 741, 499.

UV-vis (DMF): λ_{max} (ε) = 455 (2600), 482 (1300), 518 (49100), 558 (800), 660 (3300).

3.5 N-(4-hydroxyphenyl)-3,4,9,10-perylenetetracarboxylic-3,4-anhydride-9,10-imide (OHPMI)

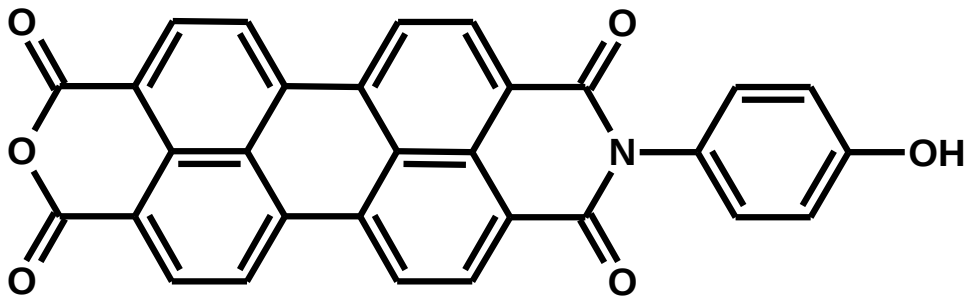

1 g (2.2 mmol) perylene-3,4,9,10-tetracarboxylic acid monohydride monopotassium carboxylate, 4-aminophenol (11.67 g) and water (50ml) were refluxed at 0-5°C for 4 hours. After that the solution was heated for 2 hours at 90°C and 12.5 ml 25% K_2CO_3 was added and refluxed at 90°C for 1 hour. The product was filtered at room temperature and washed with 2% K_2CO_3. The mixture was heated to 95°C for 5 minutes after the addition of 3.5% KOH and filtered while hot. The filtered product was acidified with 10% HCL and filtered. The crude product is purified by sublimation (-3 mbar, 300°C) according to the previously reported procedure of [9].

Yield: 74% (0.79 g, bordeaux powder).

FT-IR (KBr, cm^{-1}): ν = 3424, 3258, 3117, 2917, 1773, 1730, 1698, 1656, 1594, 1505, 1405, 1300, 1233, 1120, 1016, 807, 732.

UV-vis (DMF): λ_{max} (nm)(ε)= 453 (42700), 481 (16000), 518 (18500), 551(26400).

Fluorescence (DMF): λ_{max} (nm)= 535, 570, 622.

Fluorescence quantum yield (c =1×10^{-5} M in $CHCL_3$, refference N,N´-didodecyl-3,4,9,10-perylenebis(dicarboximide) with **Φf** = 100%, $\lambda_{excit.}$ = 485 nm)=25%.

3.6 N-(4-hydroxyphenyl)-perylene-3,4-dicarboximide-9,10-di-(isopropyloxycarbonyl) (OHPMI-Diester)

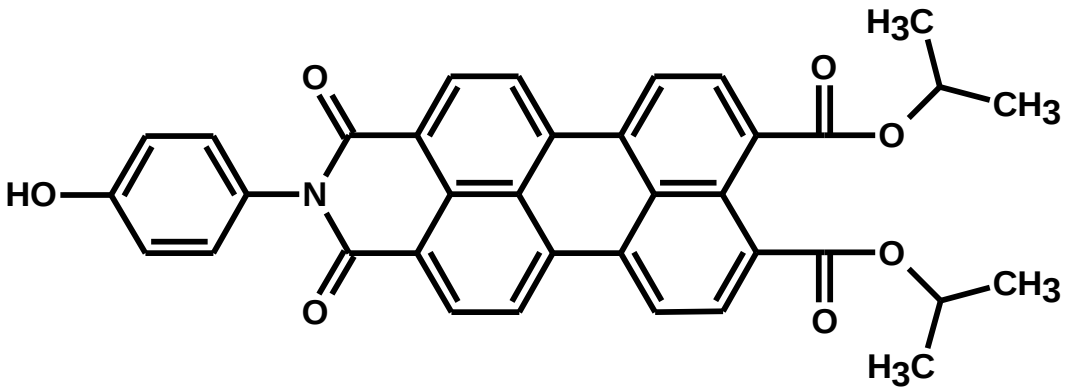

In a 2-necked round bottom flask equipped with a thermometer, condenser and magnetic stir bar, (N-(4-hydroxyphenyl)-3,4,9,10-perylenetetracarboxylic-3,4-anhydride-9,10-imide(PMI) (0.302 g, 0.625mmole)) was added to a mixture of KOH (0.169g, 3.012mmole) and isopropanol (100 ml).The solution was stirred for 30 min at room temperature. The homogeneous mixture formed was then stirred at reflux for 18h. The crude mixture was then cooled at room temperature and poured into CH_2CL_2, then it is added to aq.NH_4CL solution (PH 7) and the organic layer was extracted. After drying the organic layer over Na_2SO_4, the solution was concentrated to dryness giving a crude product of carboxylic acid perylene dye. The product was dried in vacuum oven overnight at 100°C.

Yield : 80% (321 mg); **Color** : brown ;**mp** : > 300°C.

FT-IR (KBr, cm^{-1}): ν = 3360, 3238, 3125, 2962, 2921, 2950, 1774, 1732, 1700, 1657, 1596, 1514, 1459, 1261, 1234, 1101, 1028, 833, 808, 733.

UV-vis ($CHCL_3$) λ_{max}, nm (ε_{max}, M^{-1} cm^{-1}): 451 (11900), 483 (2800), 518 (52700).

Chapter 4

DATA AND CALCULATIONS

4.1 Calculation of Fluorescence Quantum Yield (Φ_f)

The fluorescence quantum yield (QY) of a dye is the fraction of photons absorbed resulting in emission of fluorescence. It can be shown that this definition leads to:

$$\mathrm{QY} = \frac{\text{number of photons emitted}}{\text{number of photons absorbed}} = \frac{k_f}{\sum k_i}$$

Fluorescence quantum yield is an important parameter to indicate the properties of a molecule if it emits all the absorbed light or if it deactivate the absorbed light by heat. Williams et al. method is one of the well known comparative method that is used in order to calculate ϕ_f of a compound by using well standard samples that is characterized and its ϕ_f is known [43]. It is considered that, at the same excitation wavelength, both the test and standard compounds solutions have absorbed equal number of photons. The ratio of integrated fluorescence intensities of the two solutions of compounds give the quantum yield value. The unknown compound ϕ_f value is calculated by using the given equation below and a standard compound that its ϕ_f is known.

$$\Phi_f = \frac{A_{std}}{A_u} \times \frac{S_u}{S_{std}} \times \left[\frac{n_u}{n_{std}}\right]^2 \times \Phi_{std}$$

Φ_f : Fluorescence quantum yield of unknown

A_{std}: Absorbance of the reference at the excitation wavelength

A_u : Absorbance of the unknown at the excitation wavelength

S_{std}: The integrated emission area across the band of reference

S_u : The integrated emission area across the band of unknown

n_{std}: Refractive index of reference solvent

n_{std}: Refractive index of unknown solvent

Φ_{std}: Fluorescence quantum yield of reference [43, 44].

The fluorescence quantum yields of the synthesized perylene derivative were calculated by using the N,N′-bis(dodecyl)-3,4,9,10-perylenebis(discarboximide) as reference compound and it is $\Phi_f = 1$ in chloroform [44]. All the perylene derivative including the reference used in the Φ_f calculations were excited at the wavelength, $\lambda_{exc} = 485$ nm.

Φ_f calculation of OHPMI-Diester in CHL

The reference is N,N′-bis(dodecyl)-3,4,9,10-perylenebis(discarboximide) [44].

Φ_{std} = 1 in chloroform

A_{std} = 0.1055

A_u = 0.1122

S_u = 2754.12

S_{std} = 4129.22

n_{chl} = 1.446

$$\Phi f = \frac{0.1055}{0.1122} \times \frac{2754.12}{4129.22} \times \left[\frac{1.446}{1.446}\right]^2 \times 1$$

$$\Phi f = 0.63$$

Table 4.1: Fluorescence Quantum Yield of the OH-PMI and DIESTER in Chloroform.

Compound	**Solvent**	$\boldsymbol{\Phi_f}$
OH-PMI	CHL	0.25
OHPMI-Diester	CHL	0.63

4.2 Calculations of Maximum Extinction Co-efficients (ε_{max})

The linear relationship from Beer-Lambert's law gives following equation to calculate ε_{max} .

$$\boldsymbol{\varepsilon_{max} = \frac{A}{cl}}$$

Where

$\boldsymbol{\varepsilon_{max}}$ **:** Maximum extinction co-efficient in L . mol^{-1}. Cm^{-1} at λ_{max}

A **:** Absorbance

C **:** Concentration in mol L^{-1}

l **:** Path length in cm

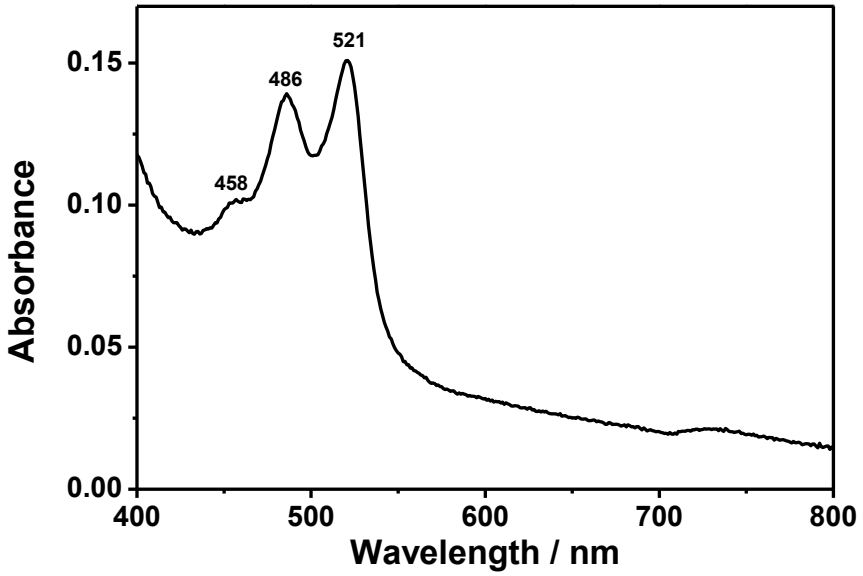

Figure 4.1: Absorption Spectrum of OHPMI- Diester in DMF at 1×10^{-5} M Concentration

According to the absorption spectrum of OHPMI-Diester (Figure 4.1) the absorption is 0.15 for the concentration of 1×10^{-5} M at the wave length, λ_{max} =521nm.

$$\boldsymbol{\varepsilon}_{\max} = \frac{0.151}{1\times10^{-5}\text{M}\times1\text{cm}} = 15100\ \text{L.mol}^{-1}.\text{cm}^{-1}$$

$$\boldsymbol{\varepsilon}_{\max}\ \text{for OHPMI} - \text{Diester} = 15100\ \text{L.mol}^{-1}.\text{cm}^{-1}$$

Table 4.2 shows the calculated molar absorptivities of all compounds.

Table 4.2: Molar Absorptivities of K-SALT, OHPMI, OHPMI-Diester

Compound	**Solvent**	**Conc. (M)**	**A**	**λ_{max} (nm)**	**ε_{max} ($M^{-1}cm^{-1}$)**
K-Salt	DMF	1×10^{-5}	0.491	518	49100
K-Salt	DMSO	1×10^{-5}	0.573	508	57300
OHP-MI	DMF	1×10^{-5}	1.685	518	18500
OHPMI-Diester	DMF	1×10^{-5}	0.151	521	15100
OHPMI-Diester	CHL	1×10^{-5}	0.527	518	52700
OHPMI Diester	MeOH	1×10^{-5}	0.264	496	26400

4.3 Calculations of Half-width of the Selected Absorption ($\Delta\overline{\nu}_{1/2}$)

The full width at half width maximum is called half-width maximum of selected wavelength.

The formula used for the calculation of $\Delta\overline{\nu}_{1/2}$ is given bellow.

$$\Delta\overline{\nu}_{1/2} = \overline{\nu}_1 - \overline{\nu}_2$$

Where

$\overline{\nu}_1, \overline{\nu}_2$: The frequencies from the absorption spectrum in cm^{-1}

$\Delta\overline{\nu}_{1/2}$: The half-width of the selected maximum absorption in cm^{-1}

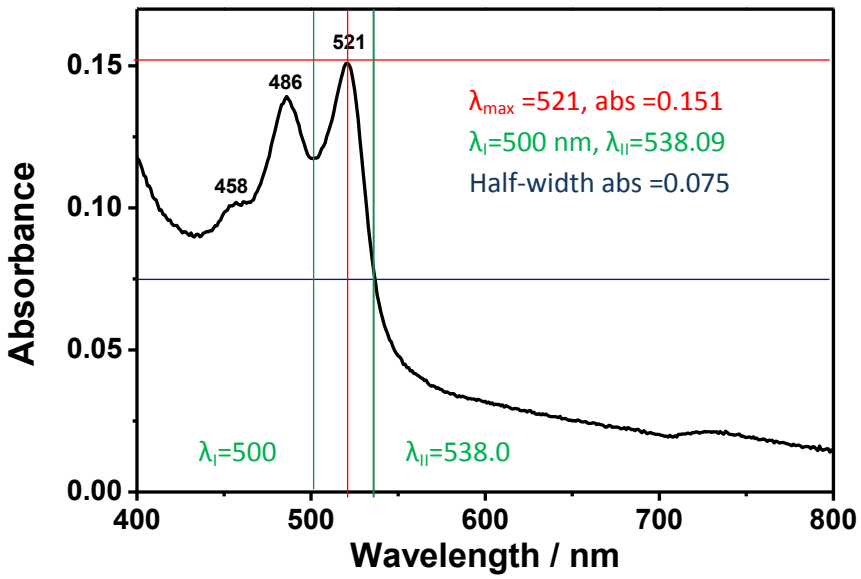

Figure 4.2: Absorption spectrum of OHPMI-Diester in DMF at 1×10^{-5} M.

According to Figure 4.2;

$\lambda_{max} = 521$ nm

Half-width absorption = 0.075

$\lambda_I = 500$ nm

$\lambda_{II} = 538.09$ nm

$$\lambda_I = 500 \text{ nm} \times \frac{10^{-9} \text{ m}}{1 \text{ nm}} \times \frac{1 \text{ cm}}{10^{-2} \text{m}} = 5 \times 10^{-5} \text{ cm}$$

$$\overline{\nu}_I = \frac{1}{5 \times 10^{-5} \text{ cm}} = 20000 \text{ cm}^{-1}$$

$$\lambda_{II} = 538.09 \text{ nm} \times \frac{10^{-9} \text{ m}}{1 \text{ nm}} \times \frac{1 \text{ cm}}{10^{-2} \text{m}} = 5.3809 \times 10^{-5} \text{ cm}$$

$$\overline{\nu}_{II} = \frac{1}{5.3809 \times 10^{-5} \text{ cm}} = 18584.25 \text{ cm}^{-1}$$

$$\Delta\overline{\nu}_{1/2} = \overline{\nu}_I - \overline{\nu}_{II} = 2000 \text{ cm}^{-1} - 18584 \text{ cm}^{-1} = 1415.75 \text{ cm}^{-1}$$

In order to calculate the theoretical radiative lifetimes of the synthesized perylene derivative, it is necessary to determine the half-widths of the compounds. As it is shown above, the half-widths were calculated for K-Salt, OH-PMI and OHPMI-Diester. All the results were listed in Table 4.3 as show below.

Table 4.3: Half-width of the Selected Absorptions of Compounds K-Salt, OH-PMI and Diester.

Compound	**Solvent**	$\boldsymbol{\lambda_{max}}$ $(\mathbf{nm})$	$\boldsymbol{\lambda_{I}}$ $(\mathbf{nm})$	$\boldsymbol{\lambda_{II}}$ $(\mathbf{nm})$	$\boldsymbol{\Delta\bar{\nu}_{1/2}}$ $(\mathbf{cm^{-1}})$
K-Salt	DMF	518	500	534.93	1273.41
K-Salt	DMSO	508	495.18	534.14	1475.43
OH-PMI	DMF	518	501	533.78	1198.28
OHPMI-Diester	DMF	521	500	538.9	1415.75
OHPMI-Diester	CHL	518	500	529.88	1096.41
OHPMI-Diester	MeOH	496	490.69	526.43	1396.76

4.4 Calculations of Theoretical Radiative Lifetime (τ_0)

The theoretical radiative lifetime is calculated by using the equation shown below. It is postulated that in the absence of nonradiative transition the theoretical lifetime of an excited molecule can be calculated as [43]

$$\boldsymbol{\tau_0 = \frac{3.5 \times 10^8}{\Delta\bar{\nu}^{\,2}_{max} \times \varepsilon_{max} \times \Delta\bar{\nu}_{1/2}}}$$

Where

$\boldsymbol{\tau_0}$**:** Theo retical radiative lifetime in ns

$\boldsymbol{\bar{\nu}_{max}}$**:** Mean frequency of the maximum absorption band in cm^{-1}

$\boldsymbol{\varepsilon_{max}}$**:** The maximum extinction co-efficient in L. mol^{-1} cm^{-1} at the maximum absorption wavelength, λ_{max}

$\boldsymbol{\Delta\bar{\nu}_{1/2}}$**:** Half-width of the selected absorption in units of cm^{-1}

Theoretical Radiative Lifetime of OHPMI-Diester:

From Figure 4.2 and 4.3,

$\lambda_{max} = 521$ nm

$$\lambda_{max} = 521 \text{ nm} \frac{10^{-9} \text{ m}}{1 \text{ nm}} \times \frac{1 \text{ cm}}{10^{-2} \text{ m}} = 5.21 \times 10^{-5} \text{cm}$$

$$\bar{\nu}_{max} = \frac{1}{5.21 \times 10^{-5} \text{cm}} = 19193.85 \text{ cm}^{-1}$$

$$\bar{\nu}^{2}_{max} = (19193.85 \text{ cm}^{-1})^2 = 3.68 \times 10^8 \text{cm}^{-2}$$

The theoretical radiative lifetime;

$$\tau_0 = \frac{3.5 \times 10^8}{\bar{\nu}^{2}_{max} \times \varepsilon_{max} \times \Delta\bar{\nu}_{1/2}} = \tau_0 = \frac{3.5 \times 10^8}{3.68 \times 10^8 \times 15100 \times 1415.75}$$

$$\tau_0 = 4.45 \times 10^{-8} \text{ s}$$

$$\tau_0 = 44.5 \text{ ns}$$

The theoretical radiative lifetimes of all the synthesized compounds K-Salt, OH-PMI and OHPMI-Diester were calculated by using the same way and all the results were listed in Table 4.4

Table 4.4: Theoretical radiative lifetimes of compounds K-Salt, OH-PMI and OHPMI-Diester

Compound	**Solvent**	$\boldsymbol{\lambda_{max}}$ $(\mathbf{nm})$	$\boldsymbol{\varepsilon_{max}}$ $(\mathbf{M^{-1}cm^{-1}})$	$\boldsymbol{\Delta\bar{\nu}^{2}_{max}}$ $\times (\mathbf{10^{8}cm^{-2}})$	$\boldsymbol{\Delta\bar{\nu}_{1/2}}$ $(\mathbf{cm^{-1}})$	$\boldsymbol{\tau_0}$ $\times (\mathbf{10^{-8}s})$
K-Salt	DMF	518	49100	3.72	1273.41	1.50
K-Salt	DMSO	508	57300	3.87	1475.43	1.07
OH-PMI	DMF	518	18500	3.72	1198.28	4.24
OHPMI-Diester	DMF	521	15100	3.68	1415.75	4.45
OHPMI-Diester	CHL	518	52700	3.72	1096.41	1.62
OHPMI-Diester	MeOH	496	26400	4.06	1396.76	2.33

4.5 Calculation of Theoretical Fluorescence Lifetime (τ_f)

The average time that a molecule stays in the excited state before fluorescence is called fluorescence lifetime. Below equation is used to calculate the theoretical fluorescence lifetime in nanosecond [45].

$$\tau_f = \tau_0 . \phi_f$$

τ_0 **:** Theoretical radiative lifetime in nano seconds

ϕ_f**:** Fluorescence quantum yield

Theoretical fluorescence lifetime calculation of OHPMI-Diester in CHL:

$$\tau_f = \tau_0 . \phi_f$$

$\tau_f = 1.62 \text{ s} \times 0.63 = 10.2 \text{ ns}$

Table 4.5 shows the theoretical fluorescence lifetime (τ_f) that was calculated for the synthesized compounds in Chloroform.

Table 4.5: Theoretical Fluorescence Lifetime (τ_f) of OHPMI-Diester in CHL.

Compound	**Solvent**	ϕ_f	τ_0 **(ns)**	τ_f **(ns)**
OHPMI-Diester	CHL	0.63	1.62	10.2

4.6 Calculation of Fluorescence Rate Constants (k_f)

The theoretical fluorescence rate constant for K-Salt, OH-PMI and OHPMI-Diester are calculated from the given equation:

$$\mathbf{K_f = \frac{1}{\tau_0}}$$

Where

$\mathbf{K_f}$: fluorescence rate constant in s^{-1}

$\boldsymbol{\tau_0}$**:** theoretical radiative lifetime in s

Fluorescence Rate Constant for OHPMI-Diester in DMF at λ_{max} = 521nm:

$$k_f = \frac{1}{4.45 \times 10^{-8}} = 2.2 \times 10^{7} s^{-1}$$

The theoretical fluorescence rate constant of all the synthesized compounds K-Salt, OH-PMI and OHPMI-Diester were calculated by using the same equation and all the results were listed in Table 4.6.

Table 4.6: Theoretical fluorescence rate constant of compounds K-Salt, OH-PMI and OHPMI-Diester

Compound	**Solvent**	**λ_{max} (nm)**	**τ_0 (s)**	**K_f (s^{-1})**
K-Salt	DMF	518	1.50×10^{-8}	6.6×10^{7}
K-Salt	DMSO	508	1.07×10^{-8}	9.3×10^{7}
OH-PMI	DMF	518	4.24×10^{-8}	2.3×10^{7}
OHPMI-Diester	DMF	521	4.45×10^{-8}	2.2×10^{7}
OHPMI-Diester	CHL	518	1.62×10^{-8}	6.1×10^{7}
OHPMI-Diester	MeOH	496	2.33×10^{-8}	4.2×10^{7}

4.7 Calculations of Oscillator Strength (f)

The strength of an electronic transition is expressed as oscillator strength which is a dimensionless quantity. The oscillator strength is calculated from the given formula

$$\mathbf{f = 4.32 \times 10^{-9} \times \Delta\bar{\nu}_{1/2} \times \varepsilon_{max}}$$

Where

f: Oscillator strength

$\mathbf{\Delta\bar{\nu}_{1/2}}$**:** Half-width of the selected absorption in units of cm^{-1}

$\boldsymbol{\varepsilon_{max}}$: Maximum extinction co-efficient in $L.mol^{-1}.\ cm^{-1}$ at λ_{max}

Oscillator strength of OHPMI-Diester in DMF at λ_{max} = 521 nm

$\mathbf{f} = 4.32 \times 10^{-9} \times \Delta\bar{\nu}_{1/2} \times \boldsymbol{\varepsilon}_{max}$

$\mathbf{f} = 4.32 \times 10^{-9} \times 1415.75 \times 15100$

$\mathbf{f} = 0.09$

The calculated oscillator strengths of the synthesized perylene derivatives K-Salt, OH-PMI and OHPMI-Diester listed in Table 4.7.

Table 4.7: Oscillator strength of the K-Salt, OH-PMI and OHPMI-Diester

Compound	**Solvent**	λ_{max} **(nm)**	$\Delta\bar{\nu}_{1/2}$ **(cm^{-1})**	ε_{max} **($M^{-1}\ cm^{-1}$)**	**ƒ**
K-Salt	DMF	518	1273.41	49100	0.27
K-Salt	DMSO	508	1475.43	57300	0.36
OH-PMI	DMF	518	1198.28	18500	0.10
OHPMI-Diester	DMF	521	1415.75	15100	0.09
OHPMI-Diester	CHL	518	1096.41	52700	0.25
OHPMI-Diester	MeOH	496	1396.76	26400	0.16

4.8 Calculations of Singlet Energy (E_s)

The amount of energy necessary for an electronic transition from ground state to excited state is called singlet energy. Singlet energy is calculated from the given formula

$$\mathbf{E_S} = \frac{\mathbf{2.86 \times 10^5}}{\boldsymbol{\lambda_{max}}}$$

Where

$\mathbf{E_s}$ **:** Singlet energy in Kcal mol^{-1}

$\boldsymbol{\lambda_{max}}$ **:** The maximum absorption wavelength in Å

Singlet energy for OHPMI-Diester in DMF at $\boldsymbol{\lambda_{max} = 521}$ nm:

$$\mathbf{E_S} = \frac{2.86 \times 10^5}{\lambda_{max}} = \frac{2.86 \times 10^5}{5210} = 54.89 \text{ Kcal mol}^{-1}$$

The singlet energies of the synthesized perylene derivatives K-Salt, OH-PMI and OHPMI-Diester listed in Table 4.8.

Table 4.8: The singlet energies of K-Salt, OH-PMI and OHPMI-Diester

Compound	Solvent	λ_{max} (Å)	E_s (Kcal.mol^{-1})
K-Salt	DMF	5180	55.21
K-Salt	DMSO	5080	56.29
OH-PMI	DMF	5180	55.21
OHPMI-Diester	DMF	5210	52.89
OHPMI-Diester	CHL	5180	55.21
OHPMI-Diester	MeOH	4960	57.66

4.9 Calculation of Optical Band Gap Energies (E_g)

LUMO and HOMO energy levels are very important parameters especially for solar cell applications. Band gap energy provides important information about LUMO and HOMO energy levels. It can be calculated by using below equation.

$$\mathbf{E_g} = \frac{\mathbf{1240\ eV\ nm}}{\boldsymbol{\lambda}}$$

Where

$\mathbf{E_g}$ **:** Band gap energy in eV

$\boldsymbol{\lambda}$ **:** Cut-off wavelength of the absorption band gap in nm

Band gap energy for OHPMI-Diester in DMF:

As shown in Figure 4.3, the cut-off wavelength of the absorption band is obtained by extrapolating the maximum absorption band to zero absorbance.

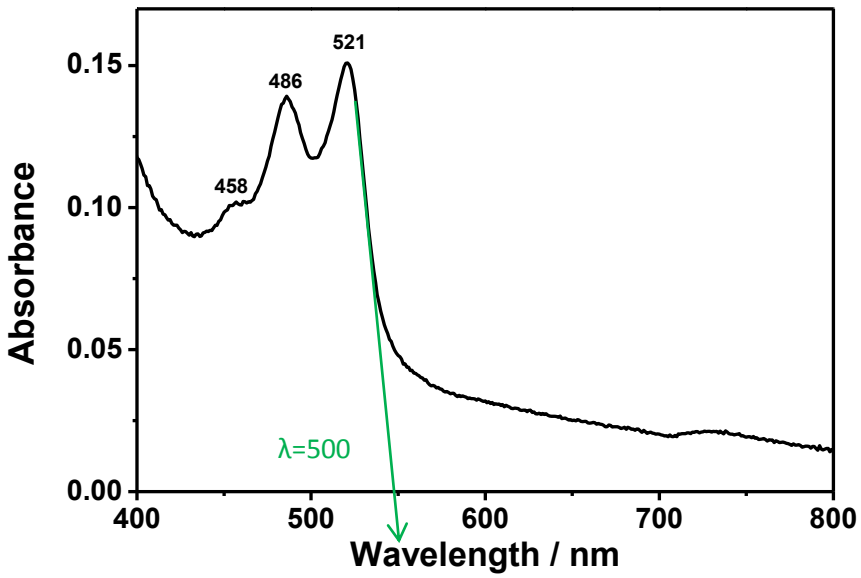

Figure 4.3: Absorption spectrum of OHPMI-Diester in DMF and the cut-off wavelength

$$E_g = \frac{1240 \text{ eV nm}}{\lambda} = \frac{1240 \text{ eV nm}}{550 \text{ nm}} = 2.25\text{eV}$$

The band gap energies of all the compounds K-Salt, OH-PMI and OHPMI-Diester were calculated by using the same equation and the calculated values are listed in Table 4.7.

Table 4.9: Band gap energies of K-Salt, OH-PMI and OHPMI-Diester

Compound	**Solvent**	**λ_{max} (nm)**	**Cut-off λ (nm)**	**E_g (eV)**
K-Salt	DMF	518	553.65	2.23
K-Salt	DMSO	508	550	2.25
OH-PMI	DMF	518	544.59	2.27
OHPMI-Diester	DMF	521	550	2.25
OHPMI-Diester	CHL	518	537.93	2.30
OHPMI-Diester	MeOH	496	552.87	2.24

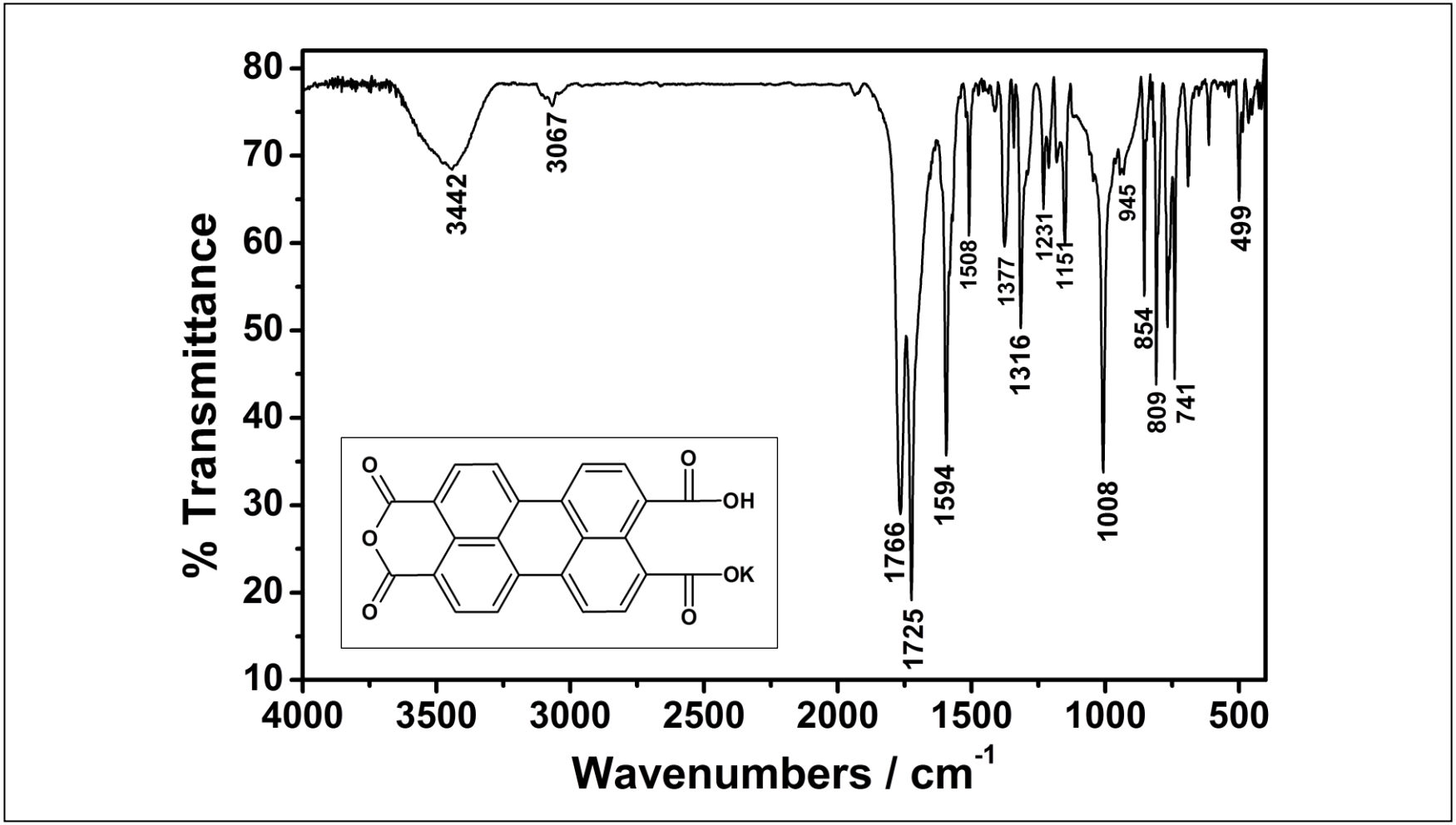

Figure 4.4: FTIR spectrum of K-SALT

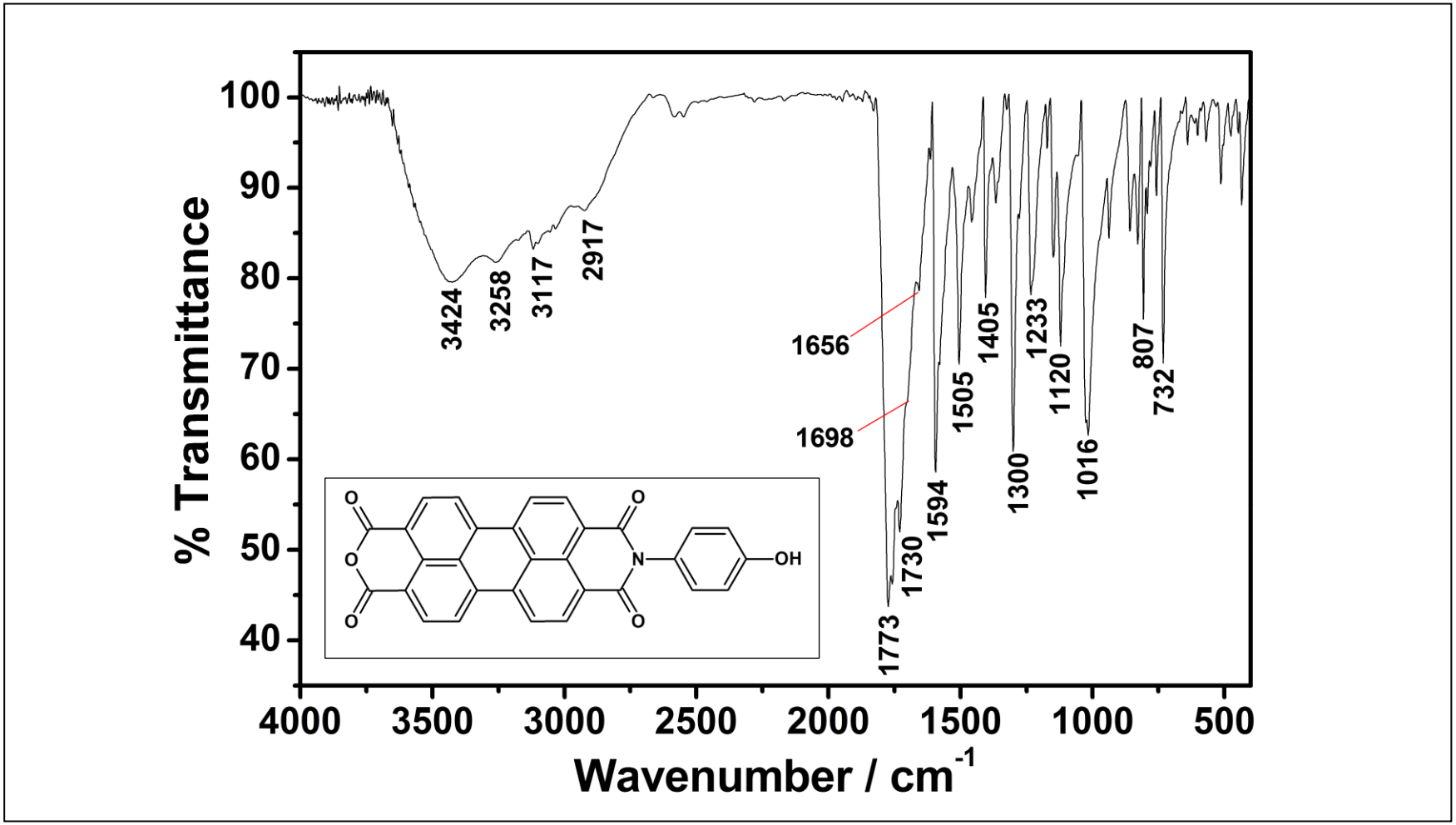

Figure 4.5: FTIR spectrum of OHPMI

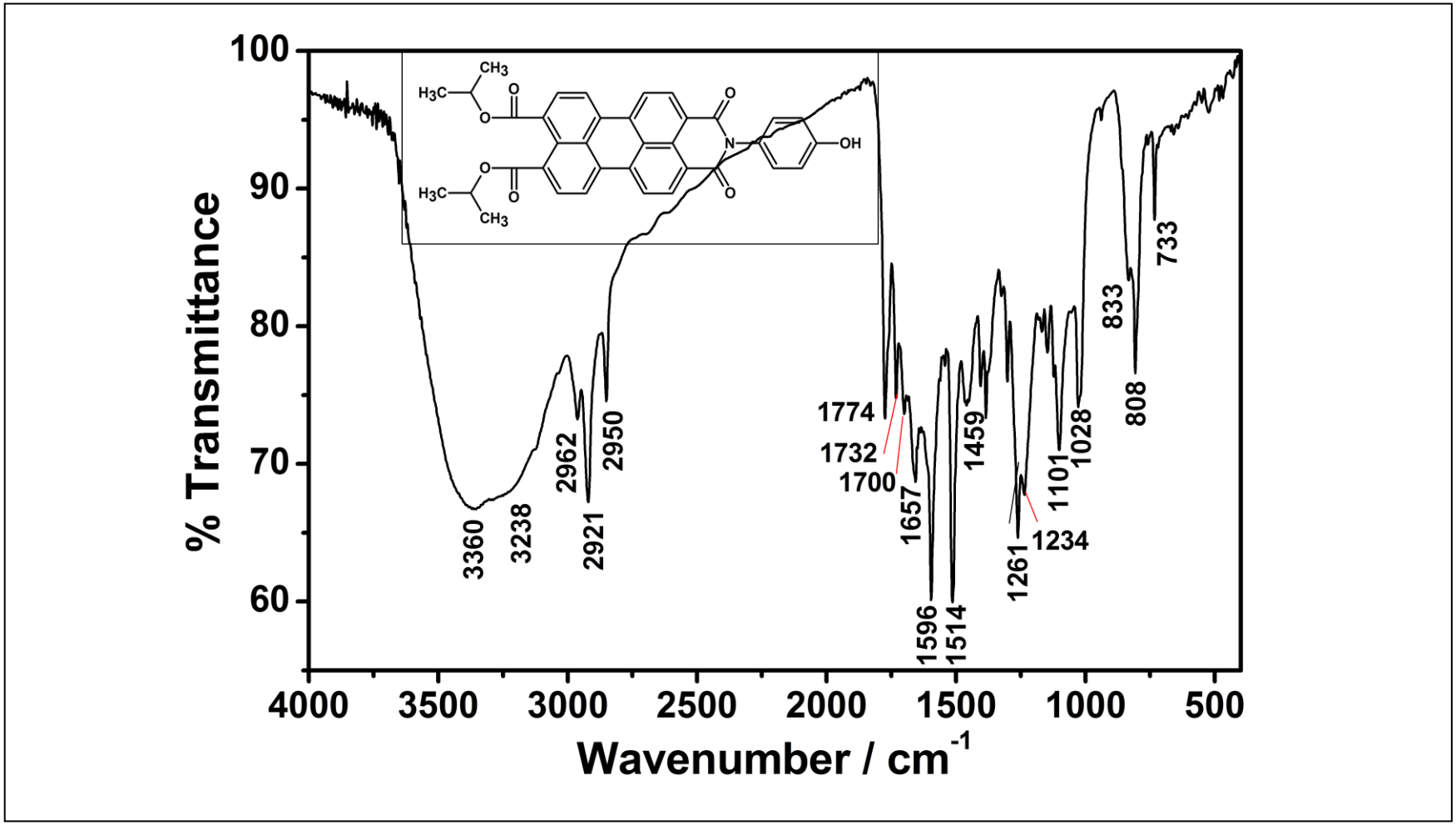

Figure 4.6: FTIR spectrum of OHPMI-DIESTER

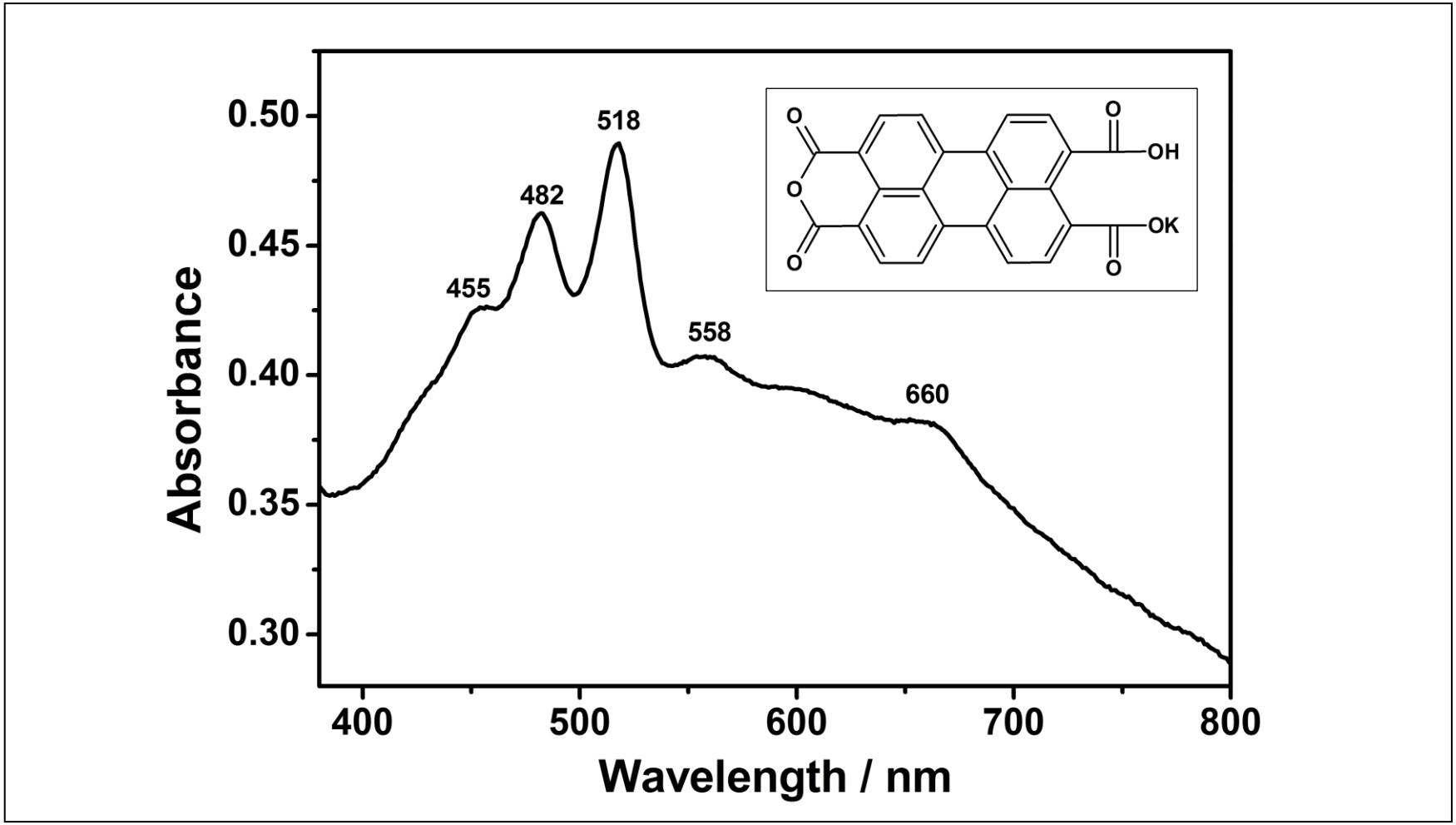

Figure 4.7: Absorbance spectrum of K-SALT in DMF

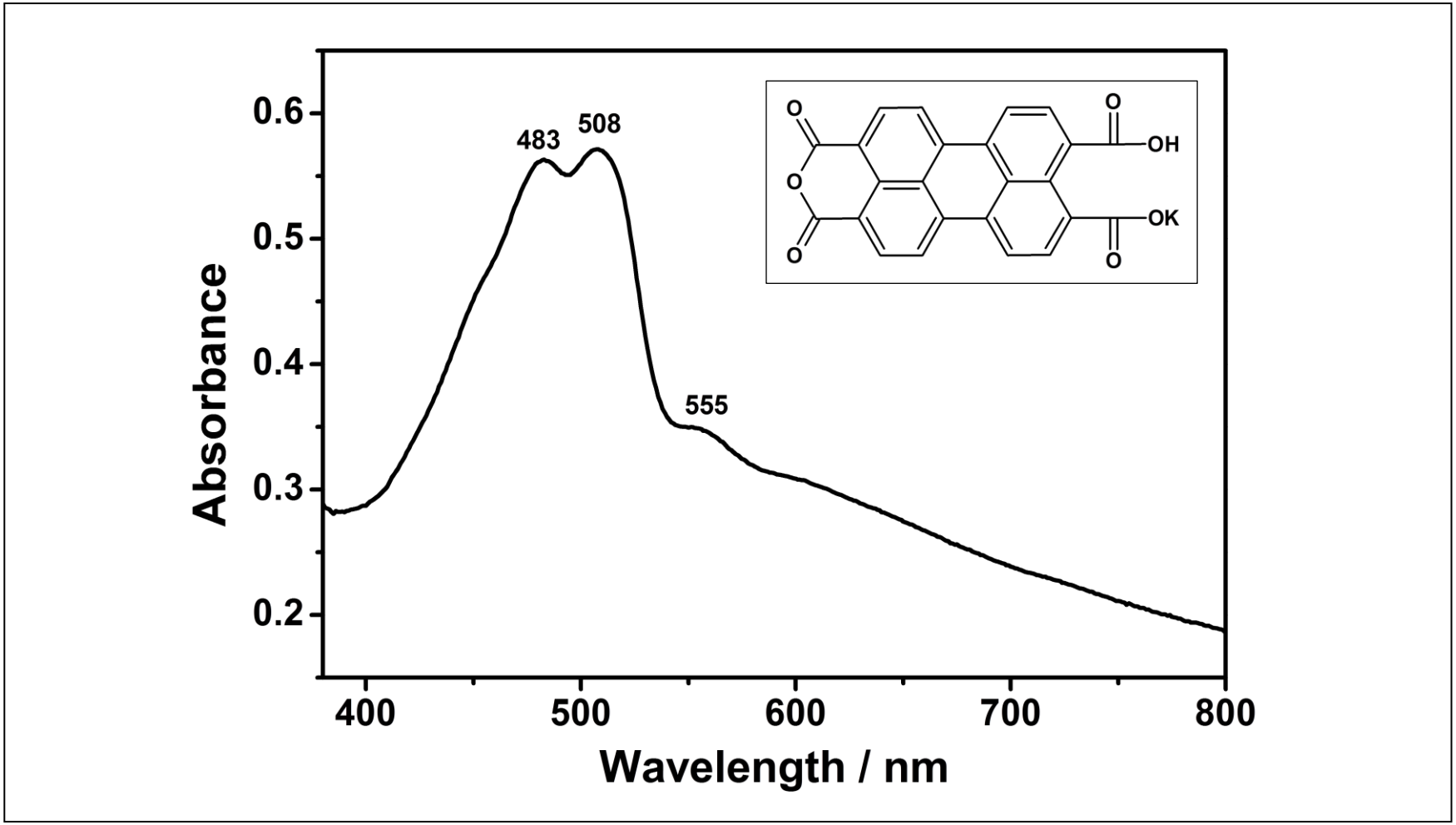

Figure 4.8: Absorbance spectrum of K-SALT in DMSO

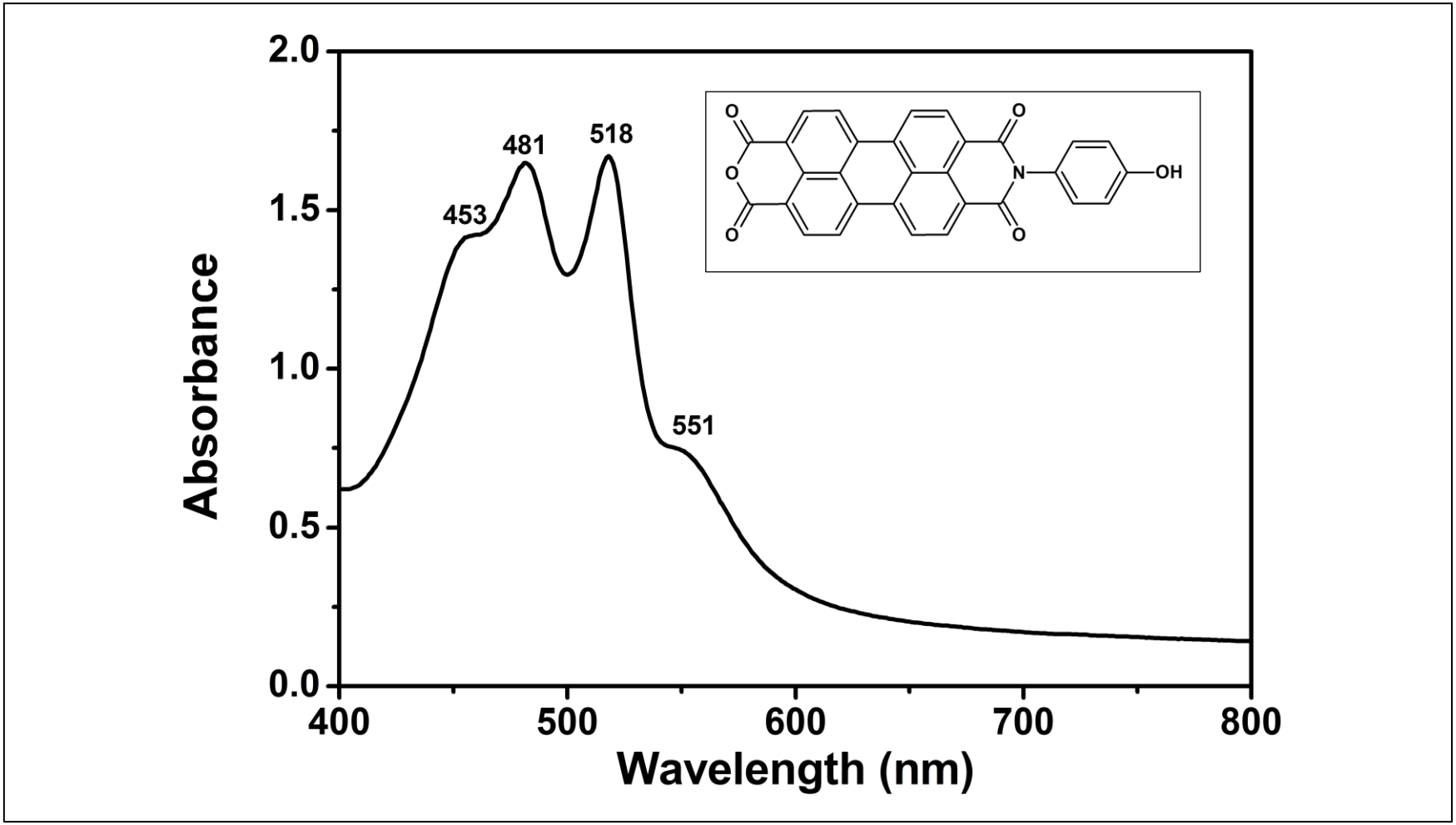

Figure 4.9: Absorbance spectrum of OHPMI in DMF

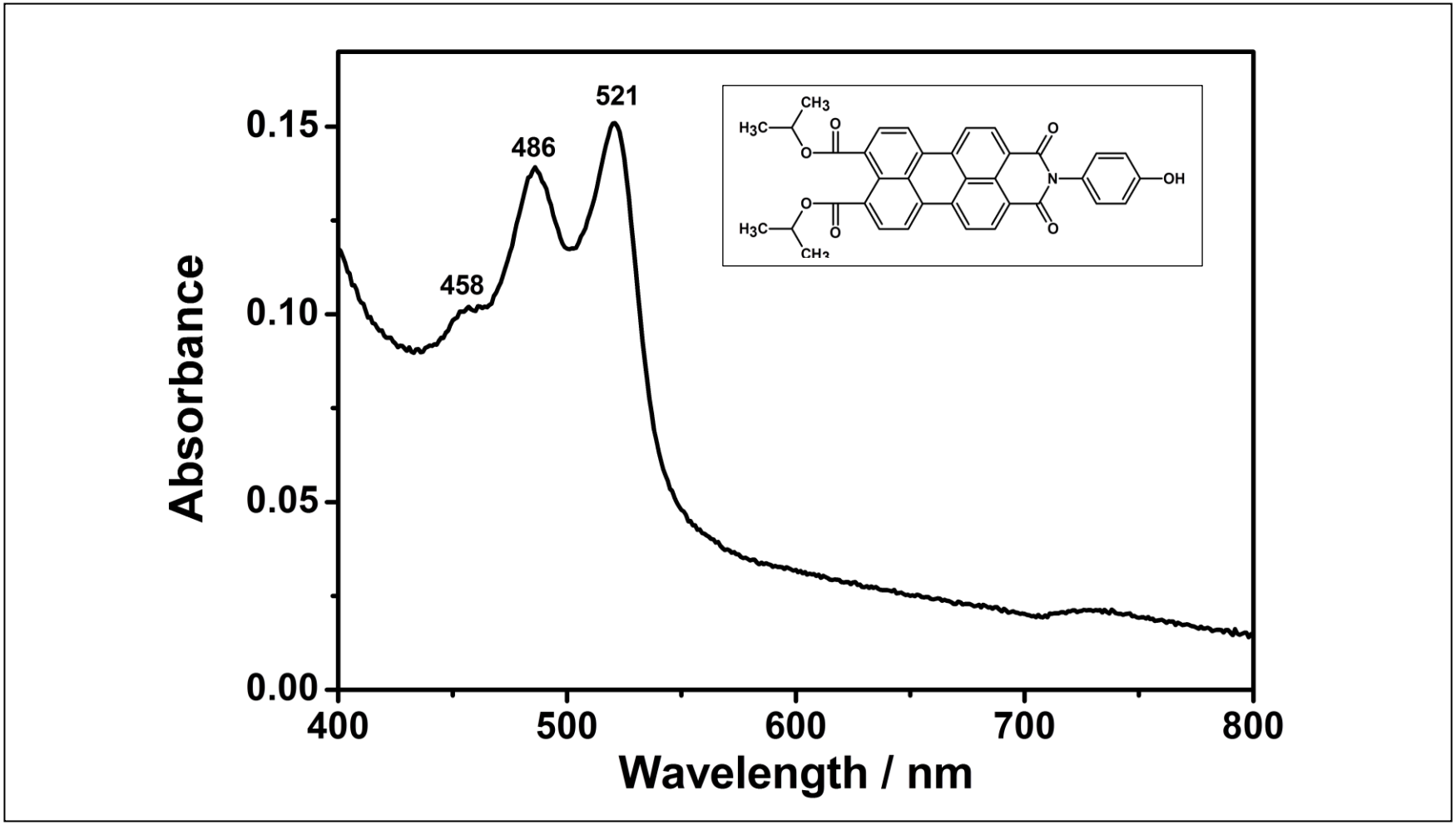

Figure 4.10: Absorbance spectrum of OHPMI-DIESTER in DMF

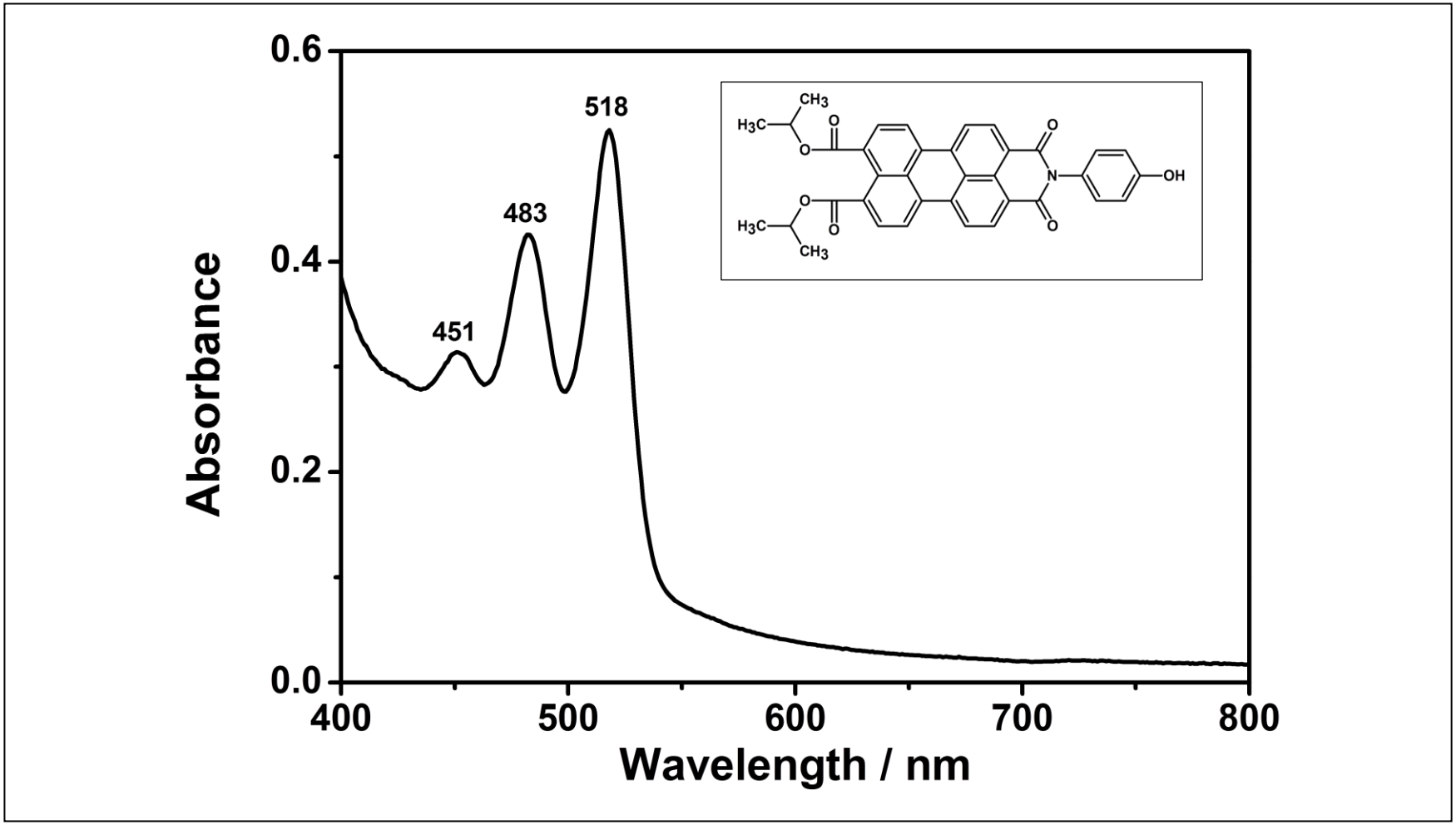

Figure 4.11: Absorbance spectrum of OHPMI-DIESTER in CHL

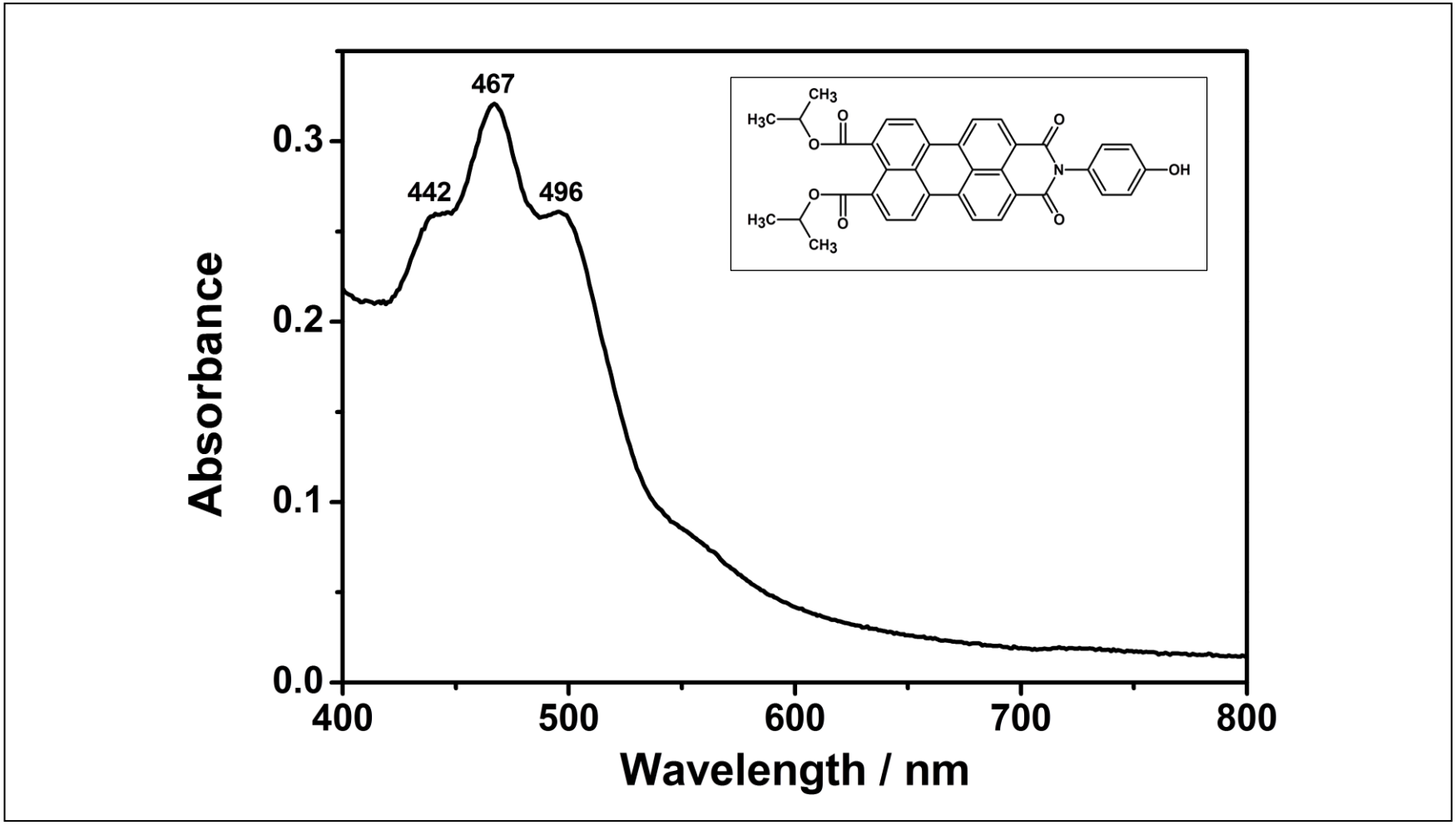

Figure 4.12: Absorbance spectrum of OHPMI-DIESTER in MeOH

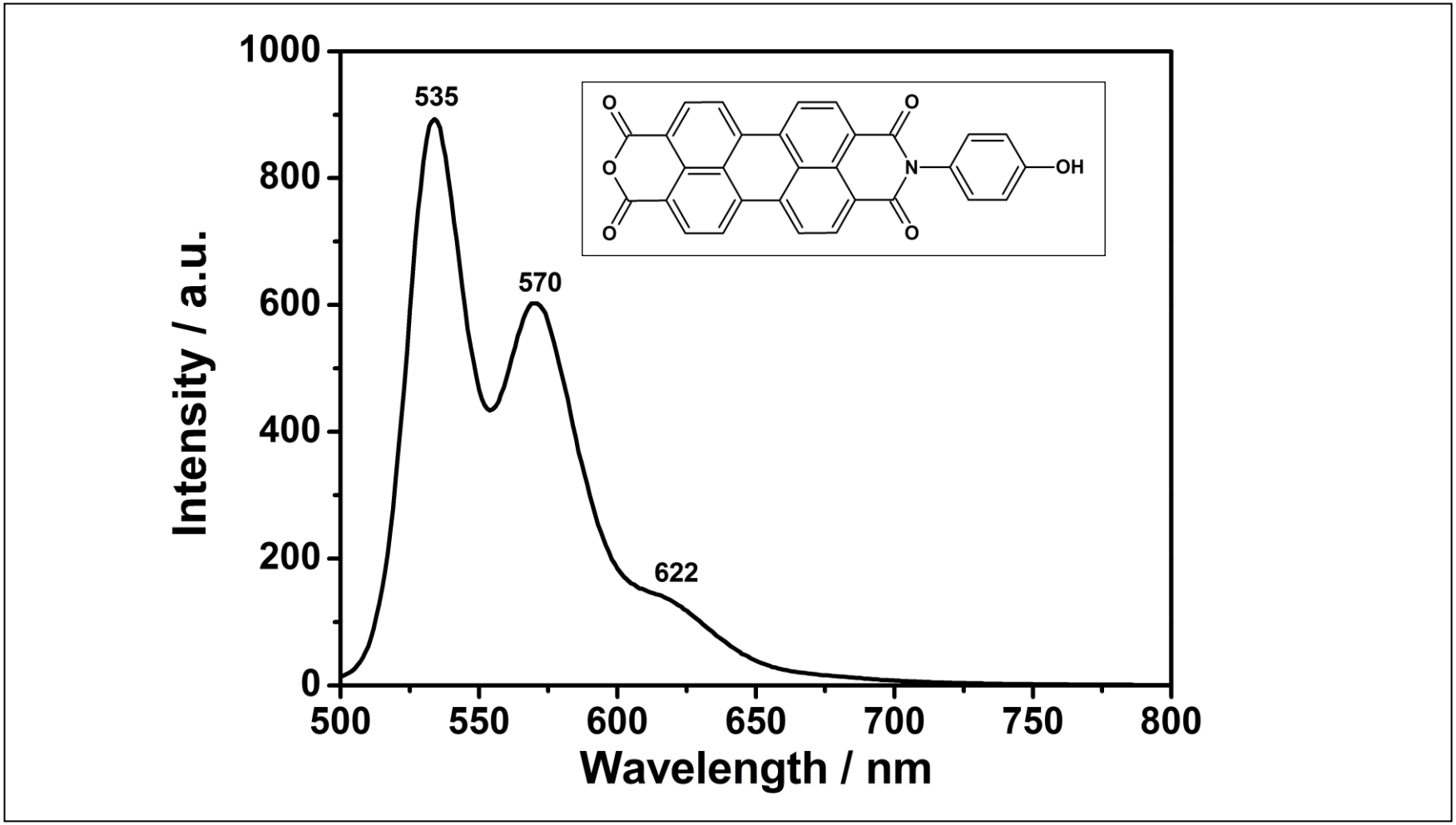

Figure 4.13: Emission spectrum of OHPMI in DMF

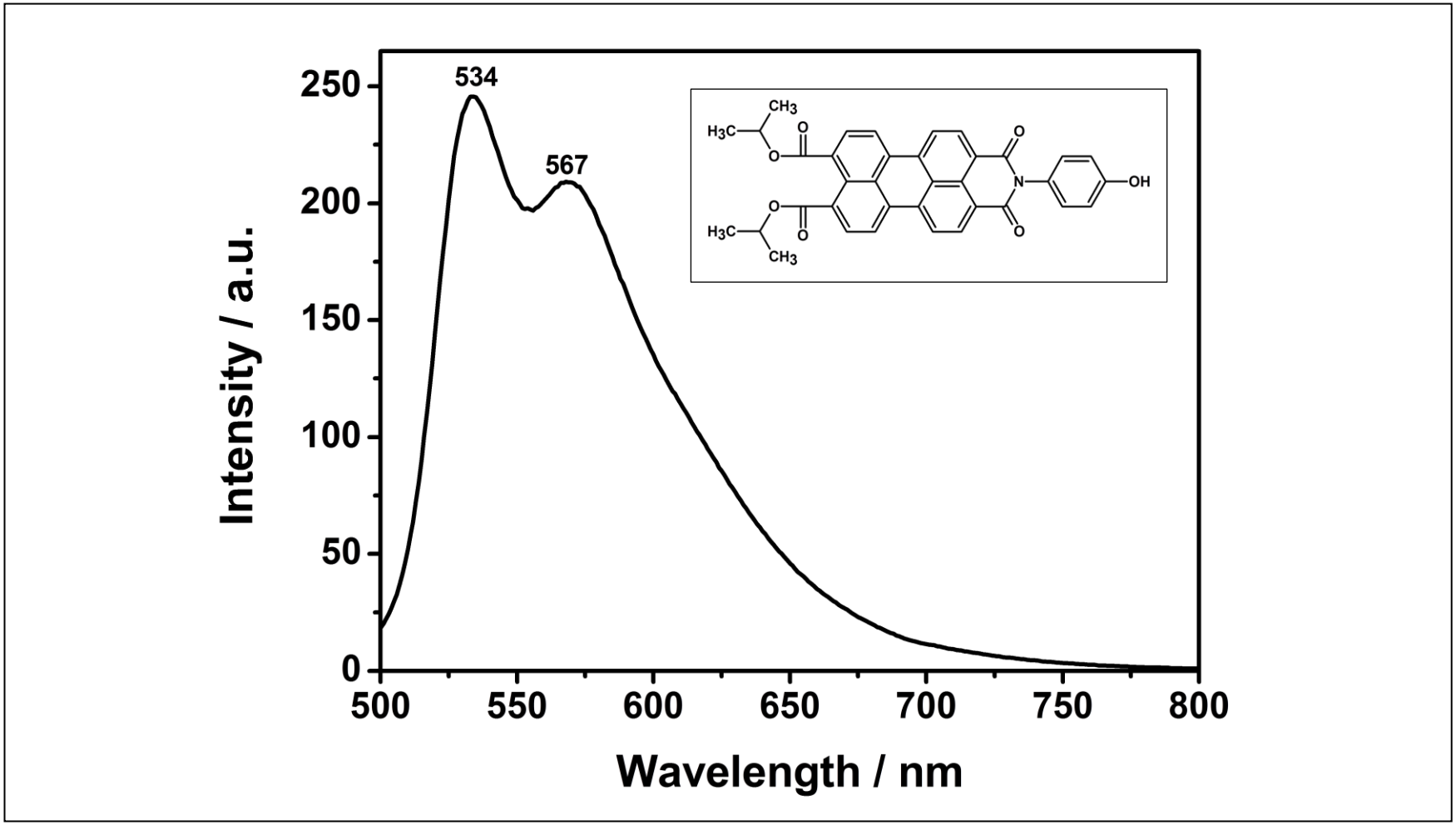

Figure 4.14: Emission spectrum of OHPMI-DIESTER in DMF

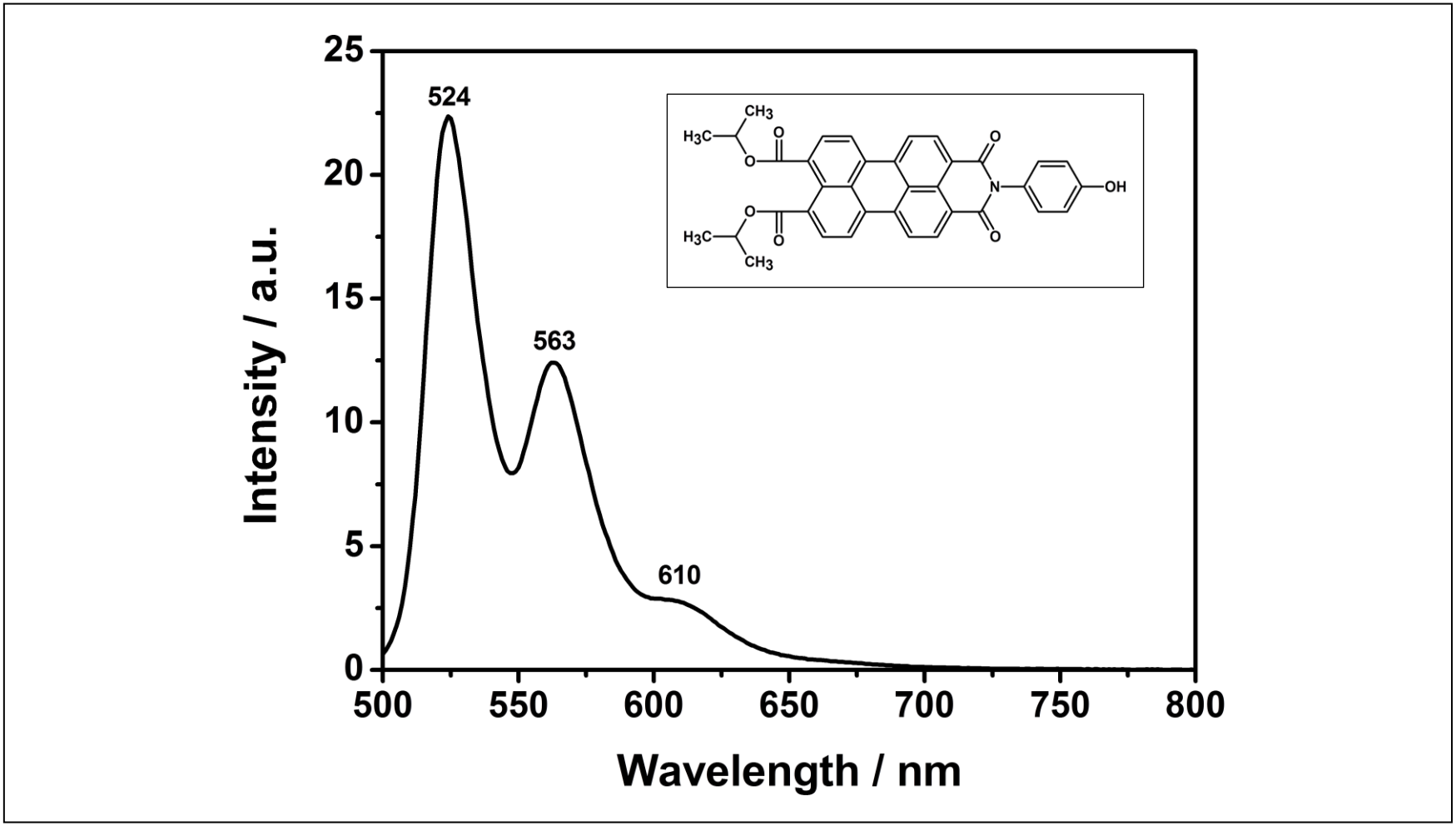

Figure 4.15: Emission spectrum of OHPMI-DIESTER in CHL

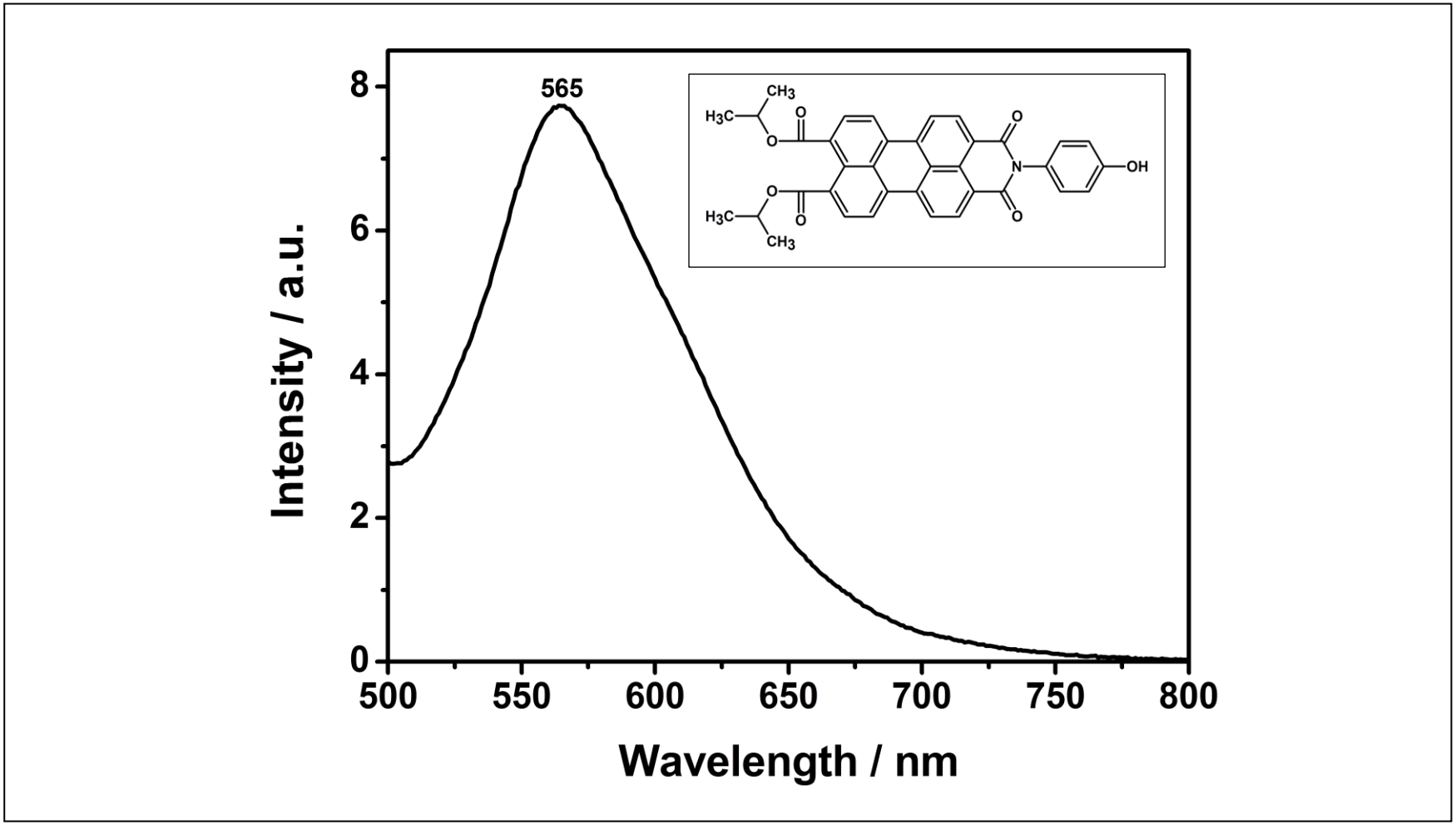

Figure 4.16: Emission spectrum of OHPMI-DIESTER in MeOH

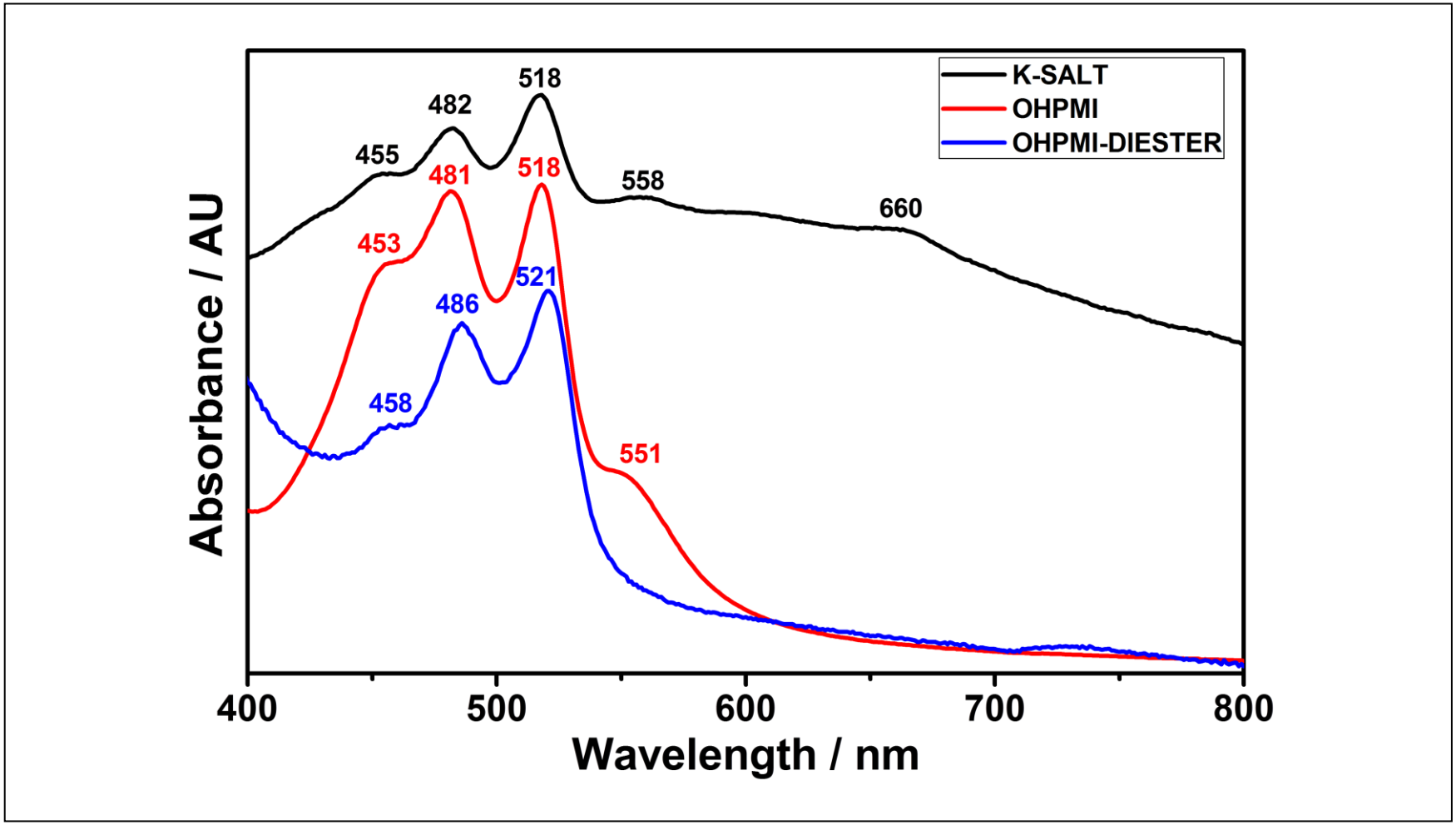

Figure 4.17: Absorption spectra of K-SALT, OHPMI and OHPMI-DIESTER in DMF

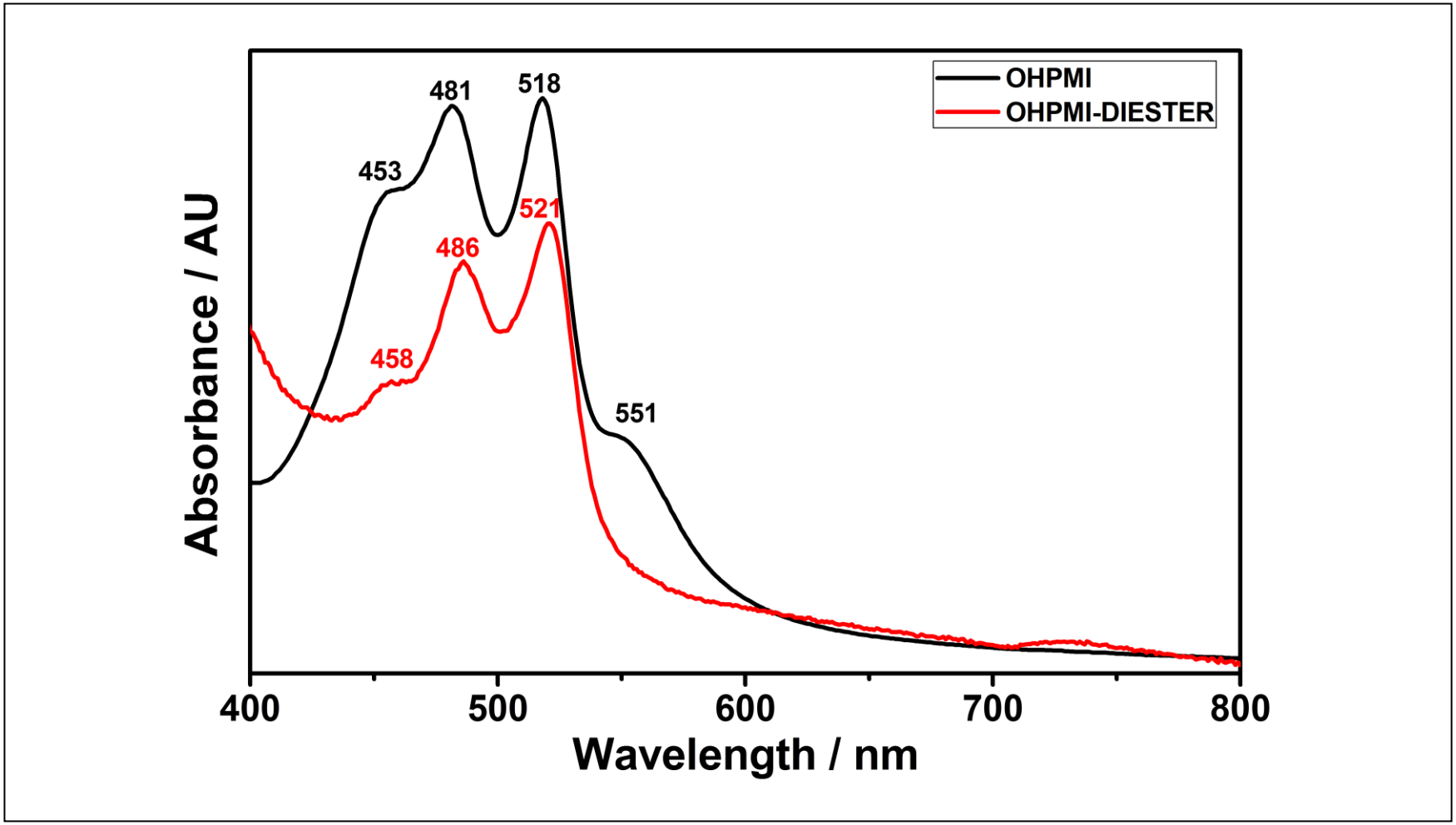

Figure 4.18: Absorption spectra of OHPMI and OHPMI-DIESTER in DMF

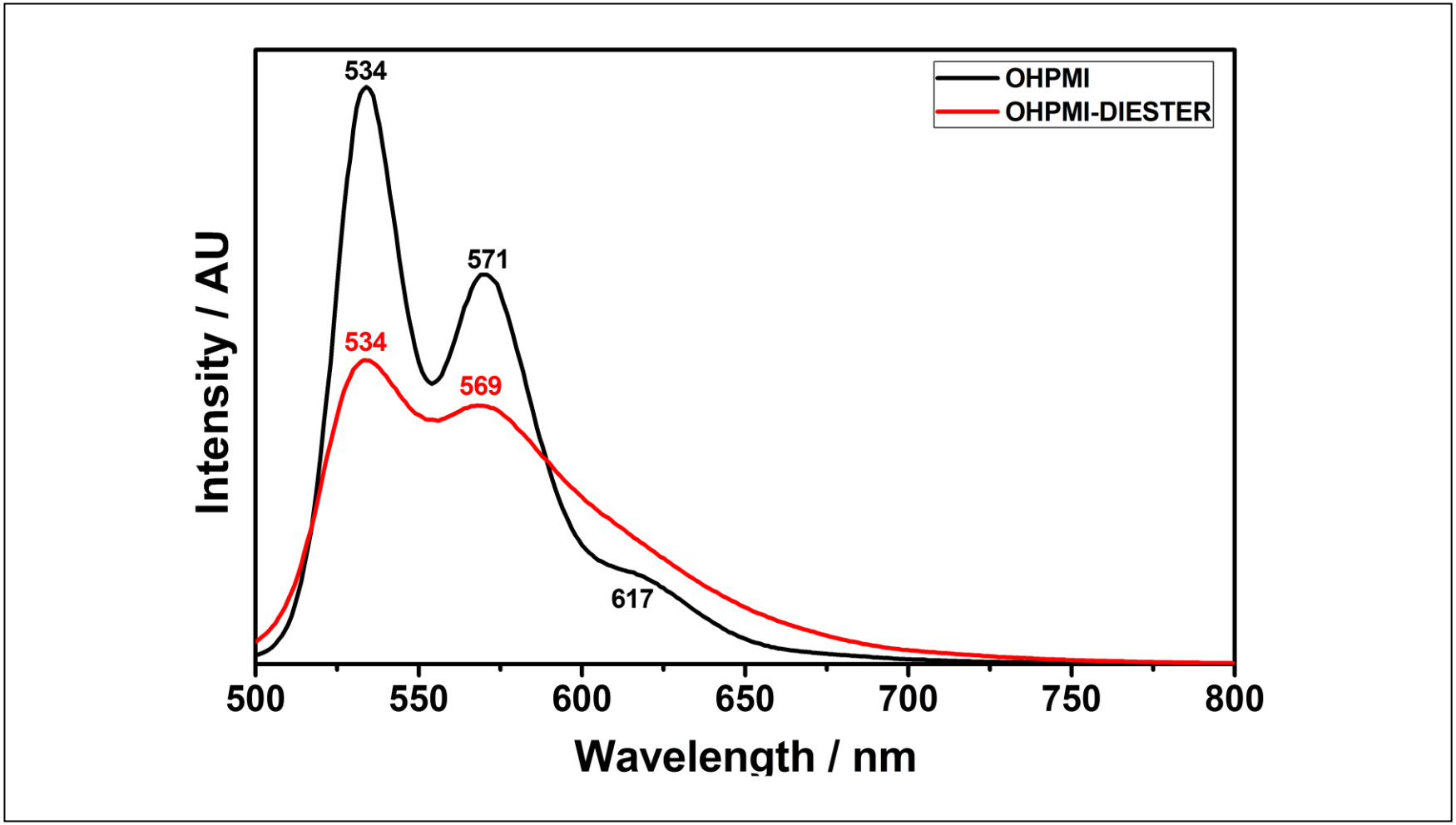

Figure 4.19: Emission spectra of OHPMI and OHPMI-DIESTER in DMF

Chapter 5

RESULTS AND DISCUSSION

5.1 Syntheses of the Designed Perylene Dyes

Perylene chromophoric ligands are designed for DNA binding. The chemical structure of all the synthesized derivatives and synthetic pathway are illustrated in Scheme 1.1. Starting from perylene-3,4,9,10-tetracarboxylic acid dianhydride (PDA) perylene-3,4,9,10-tetracarboxylic acid monoanhydride monopotassium carboxylate (K-Salt),was first prepared which is followed by the preparation of N-(4-hydroxyphenyl)-3,4,9,10-perylenetetracarboxylic-3,4-anhydride-9,10-imide (OHPMI) and finally N-(4-hydroxyphenyl)-perylene-3,4-dicarboximide-9,10-di-(isopropyloxycarbonyl) (OHPMI-Diester) is prepared for DNA binding.

In the first step, the starting material perylene dianhydride (PDA) was converted to a Perylene-3, 4,9,10-tetracarboxylic acid monoanhydride monopotassium carboxylate (K-SALT) in presence of KOH and phosphoric acid then in the second step, the synthesis of Perylene-3,4,9,10-tetracarboxylic acid monoanhydride monopotassium carboxylate (K-SALT) was converted to N-(4-hydroxyphenyl)-3,4,9,10-perylenetetracarboxylic-3,4-anhydride-9,10-imide (OHPMI) in presence of 4-aminophenol and finally in the third step, the synthesis of N-(4-hydroxyphenyl)-3,4, 9,10-perylenetetracarboxylic-3 ,4-anhydride-9, 10-imide (OH-PMI) was converted to N-(4-hydroxyphenyl)-perylene-3,4-dicarboximide-9,10-di-(isopropyloxycarbonyl) (OHPMI-DIESTER) in the presence of isopropanol. The yield of the products were

quite high[9] where the yield of the synthesized OH-PMI-Diester is 80% , K-Salt is 89% and OH-PMI is 74% as great care was taken to complete the reaction by means of a continuous monitoring of the reaction progress through thin layer chromatography (TLC) and FTIR techniques.

5.2 Solubility of the Synthesized Perylene Derivative

The newly synthesized OHPMI-Diester is completely soluble in chloroform and methanol where it is partly soluble in DMF at room temperature. As the temperature increases the solubility of OH-PMI in DMF increases.

Appreciable solubility was achieved in protic solvents such as methanol, DMF and CHL. The solubility properties of the products are tabulated in table 5.1. One of the interesting properties noticed for OHPMI-Diester in DMF is that it is very fluorescence. In DMF the high solubility combined with fluorescent colors indicates a potential for a wide range of applications in industry.

Table 5.1: Solubility of OHPMI-Diester

Solvent	**Solubility***	**Color**
CHL	(+ +)	Orange
MeOH	(+ +)	Dark orange
DMF	(– +)	Light pink

(+ +): Completely soluble;(– +): Partially soluble; (– –): Insoluble ; *:Solubility increase on heating

5.3 Analysis of FTIR Spectra

All the synthesized perylene dye compounds were basically characterized by FTIR spectra for the conformation of functional groups present in the structures. The spectra completely represented the basic functional groups present in their structure. The peaks observed from the FTIR spectra are described below.

From Figure 4.4, broad carboxylic O-H stretching at 3442 cm^{-1}, aromatic C- H stretch at 3067 cm^{-1}, anhydride carbonyl (C=O) stretching at 1766 and 1725 cm^{-1}, conjugated C=C stretching at 1594, C-O stretching at 1008 cm^{-1}, aromatic C-H bend at 809 and 741 cm^{-1}.

From Figure 4.5, OH phenol at 3424 cm^{-1}, aromatic C-H at 3117 cm^{-1}, anhydride carbonyl C=O stretching 1773 and 1730 cm^{-1}, imide carbonyl N-C=O stretching at 1698 and 1656 cm^{-1}, conjugated C=C stretching at 1594 cm^{-1}, C-N stretch at 1300 cm^{-1}, C-O stretching at 1016 cm^{-1}, aromatic C-H bend at 807 and 732 cm^{-1} confirm the structure of PMI.

From Figure 4.6, broad phenol O-H stretch at 3360 cm^{-1}, aromatic C-H at 3125 cm^{-1}, aliphatic C-H stretch at 2921 and 2950 cm^{-1}, ester C=O stretch at 1774 and 1732 cm^{-1}, C=O imide at 1700 and 1657 cm^{-1}, conjugated C=C stretching at 1596 cm^{-1}, ester C-O stretch at 1261and 1234 cm^{-1}, C-O stretching at 1028 cm^{-1}, aromatic C-H bend at 808 and 733 cm^{-1} confirms the structure of OHPMI-Diester.

5.4 Interpretation of UV-vis Spectra

Figure 4.7-4.8 show the absorption spectra of K-Salt in various solvents. All the absorption spectra recorded for K-Salt represented three characteristic absorption peaks at 455, 482, and 518 nm in DMF and 483, 508, and 555 nm in DMSO relating to conjugated perylene chromophoric π-π interactions. Table 4.2 suggests the high molar extinction coefficient (ε_{max} = 49100 M^{-1} cm^{-1}) in DMF and (ε_{max} = 57300 M^{-1} cm^{-1}) in DMSO of K-Salt inferring strong absorption in the visible region. Table 4.7 and 4.8 also represents the strong possibility for singlet electronic excitation from ground state.

Figure 4.9 shows the absorption spectra of OH-PMI in DMF solvent. The absorption spectra recorded for PMI representes three characteristic absorption peaks at 453, 481, and 518 nm relating to conjugated perylene chromophoric π-π interactions. Table 4.2 suggests the moderate molar extinction coefficient (ε_{max} = 18500 M^{-1} cm^{-1}) of PMI inferring strong absorption in the visible region. Table 4.7 and 4.8 also represent the strong possibility for singlet electronic excitation from ground state.

Figures 4.10-4.12 shows the absorption spectra of OHPMI-Diester in various solvents. All the absorption for OHPMI-Diester represents three characteristic absorption peaks. As it is shown in Table 5.2 which is relating to conjugated perylene chromoforic (π-π) interactions.

Table 5.2: The UV-vis absorption wavelengths for OHPMI-Diester at (1×10^{-5} M).

Solvent	**UV-vis (nm)**
DMF	458, 486, 521
CHL	451, 483, 518
MeOH	442, 467,456

Table 4.2 suggests the molar excitation coefficient (ε_{max} = 15100 M^{-1} cm^{-1}) in DMF, the high molar excitation coefficient (ε_{max} = 52700 M^{-1} cm^{-1}) in CHL and the high molar excitation coefficient (ε_{max} = 24600 M^{-1} cm^{-1}) in MeOH of OHPMI-Diester inferring strong absorption in the visible region. Table 4.7 and 4.8 also represents the strong possibility for singlet electronic excitation from ground state. Comparing to K-Salt, OH-PMI; OHPMI-Diester has not shown noticeable change in terms of ε_{max}.

Figure 4.17 shows the absorption spectra of K-Salt, OH-PMI and OHPMI-Diester in DMF. They are similar with the traditional three peaks and no considerable changes were noticed in the three reported compounds.

Figure 4.18 shows the absorption spectra of OH-PMI and OHPMI-Diester in DMF. they are similar with the traditional three peaks and no considerable changes were noticed in the two reported compounds.

5.5 Interpretation of Emission Spectra

Figure 4.13 shows the emission spectra of OH-PMI in DMF which represented three characteristic emission peaks at 535, 570 and 622 nm relating to conjugated perylene chromophoric (π-π) interactions.

Figure 4.19 shows the emission spectra of OH-PMI and OHPMI-Diester in DMF solvent are similar in peak shapes and the three perylene emission peaks were noticed.

Figure 4.14 shows the emission spectra of OHPMI-Diester in DMF. Which represented two characteristic emission peaks at 534 and 567 nm relating to conjugated perylene chromophoric π-π interactions.

Figure 4.15 shows the emission spectra of OHPMI-Diester in CHL . The emission spectra for OHPMI-Diester represented three characteristic emission peaks at 524, 563 and 610 nm relating to conjugated perylene chromophoric π-π interactions.

Figure 4.16 shows the emission spectra of OHPMI-Diester in MeOH. The emission spectra for OHPMI-Diester represents one characteristic emission peak at 565 nm relating to conjugated perylene chromophoric π-π interactions.

Figure 4.17 shows the emission spectra of K-Salt, OH-PMI and OHPMI-Diester in DMF solvents are similar in peak shapes and the three perylene emission peaks were noticed.

Chapter 6

CONCLUSION

Perylene-3,4, 9,10-tetracarboxylic acid monoanhydride monopotassium carboxylate (K-SALT), perylene monoimide (OH-PMI) and N-(4-hydroxyphenyl)-perylene-3,4-dicarboximide-9, 10-di-(isopropyloxycarbonyl) (OHPMI-DIESTER) synthesized and charecterized sucessfully.

The three perylene derivatives are soluble in common organic solvents.

The FTIR spectrum confirms the basic functional groups present in the structures and confirm the purity of the sample.

The absorption spectra of all perylene derivatives exhibited three traditional perylene chromophoric absorption peaks.

The UV-vis absorption spectra recorded in various category of solvents (DMF, CHL, and MeOH) suggest moderate absorption ability of the compounds. Particularly, OHPMI-Diester has shown moderate molar absorpitivity of ε_{max} = 15100 M^{-1} cm^{-1} in dimethyle formamide (DMF) ε_{max} = 52700 M^{-1} cm^{-1} in chloroform (CHL), and ε_{max} = 26400 M^{-1} cm^{-1} in methanol (MeOH).

The emission spectra recorded for OHPMI-Diester have shown the characteristic three emission peaks in all type of solvents.

REFERENCES

[1] Langhals, H. (1995). Heterocycles. 40, 477-500.

[2] Hunger, K., and Herbst, W. (1987). Zndustrielle Organische Pigmente: Herstellung, Eigenschaften, Anwendungen, 1 st ed., VCH Verlagsgesellschaft mbH, Weinheim.

[3] Krasovitskii, B. M., and Bolotin, B. M. (1988). Organic Luminescent Materials,1 st ed., VCH Verlagsgesellschaft, Weinheim.

[4] Czajkowski, W. S., Peters, A. T., and Freeman, H. S. (1995). Modern Colorants, Synthesis and Structure, Chapman & Hall, New York.

[5] Zollinger, H. (1991). Color Chemistrv. 2nd ed., VCH Verla-gs-ge sellschaft, Wgnheim.

[6] Feiler, L., Lanehals, H., and Polborn, K. (1995). Liebias Ann. I, 1229- 1244.

[7] Türkmen, G., Erten-Ela, S., and Icli, S. (2009). Highly soluble perylene dyes: Synthesis, photophysical and electrochemical characterizations. Dyes and Pigments. 83, 297–303.

[8] Kaur, B., Bhattacharya, S. N., and Henry, D. J. (2013). Interpreting the near-infrared reflectance of a series of perylene pigments. Dyes and Pigments. 99, 502-511.

[9] Pasaogullari, N., Icil, H., and Demuth, M. (2006). Symmetrical and unsymmetrical perylene diimides: Their synthesis, photophysical and electrochemical properties. Dyes and Pigments. 69, 118-127.

[10] Dincalp, H., Avcıbası, N., and Icli, S. (2007). Spectral properties and G-quadruplex DNA binding selectivities of a series of unsymmetrical perylene diimides. Journal of Photochemistry and Photobiology A: Chemistry. 185, 1–12.

[11] Wang, R., Shi, Z., Zhang, C., Zhang, A., Chen, J., Guo, W., and Sun, Z. (2013). Facile synthesis and controllable bromination of asymmetrical intermediates of perylene monoanhydride/monoimide diester. Dyes and Pigments. 98, 450-458.

[12] Tomizaki, K., Thamyongkit, P., Loewe, R. S., and Lindsey, J. S. (2003). Practical synthesis of perylene-monoimide building blocks that possess features appropriate for use in porphyrin-based light-harvesting arrays. Tetrahedron. 59, 1191–1207.

[13] Feiler, L., Langhals, H., and Polborn, K. (1995). Liebigs Ann. 1229–1244.

[14] Quante, H., and Müllen, K. (1995). Angew. Chem. Int. Ed. Engl. 34, 1323–1325.

[15] Holtrup, F. O., Müller, G. R. J., Quante, H., De Feyter, S., De Schryver, F. C., and Müllen, K. (1997). Chem. Eur. J. 3, 219–225.

[16] Müller, G. R. J., Meiners, C., Enkelmann, V., Geerts, Y., and Müllen, K. (1998). J. Mater. Chem. 8, 61–64.

[17] Gosztola, D., Niemczyk, M. P., and Wasielewski, M. R. (1998). J. Am. Chem. Soc. 120, 5118–5119.

[18] Fuller, M. J., and Wasielewski, M. R. (2001). J. Phys. Chem. B. 105, 7216–7219.

[19] Just, E. M., and Wasielewski, M. R. (2000). Superlatt. Microstruct. 28, 317–328.

[20] Hayes, R. T., Wasielewski, M. R., and Gosztola, D. J. (2000). Am. Chem. Soc. 122, 5563–5567.

[21] Lukas, A. S., Zhao, Y., Miller, S. E., and Wasielewski, M. R. (2002). J. Phys. Chem. B. 106, 1299–1306.

[22] Emtiazi G. (2007) Introduction of molecular biology and genetic engineering, Mani publication, Tehran.

[23] Islam, M., Chakraborty, M., Pandya, P., Al Masum, A., Gupta, N., and Mukhopadhyay, S. (2013). Binding of DNA with Rhodamine B: Spectroscopic and molecular modeling studies. Dyes and Pigments. 99, 412-422.

[24] Zhao, C., and Qu, X. (20 13). Recent progress in G-quadruplex DNA in deep eutectic solvent. Methods. 64, 52–58.

[25] Chen, S., Shi, Q., Peng, D., Huang, S., Ou, T., Li, D., Tan, J., Gu, L., and Huang, Z. (2013). The role of positive charges on G-quadruplex binding small molecules: Learning from bisaryldiketene derivatives. Biochimica et Biophysica Acta. 1830, 5006–5013.

[26] Asir, S., Demir, A. S., and Icil, H. (2010). The synthesis of novel, unsymmetrically substituted, chiral naphthalene and perylene diimides: Photophysical, electrochemical, chiroptical and intramolecular charge transfer properties. Dyes and Pigments. 84, 1–13.

[27] Rescifina, A., Zagni, C., Varrica, M. G., Pistarà, V., and Corsaro, A. (2014). Recent advances in small organic molecules as DNA intercalating agents: Synthesis, activity, and modeling. European Journal of Medicinal Chemistry. 74, 95-115.

[28] Burge, S., Parkinson, G. N., Hazel, P., Todd, A. K., and Neidle, S. (2006). Quadruplex DNA: sequence, topology and structure. Quadruplex DNA: sequence, topology and structure. Nucleic Acids Res. 34 (19), 5402–5415.

[29] Steullet, V., Dixon, D. W., Takenaka, S., and Wilson, W. D. (1997). Studies of Naphthalene Diimides as DNA-binding Agents. First International Electronic Conference on Synthetic Organic Chemistry (ECSOC-1), 1-30.

[30] Bhosale, S. V., Janiab, C. H., and Langford, S. (2008). Chemistry of naphthalene diimides. Chemical Society Reviews. 37, 331–342.

[31] Lin, C., Velusamy, M., Chou, H., Lin, J. T., and Chou, P. (2010). Synthesis and characterization of naphthalene diimide (NDI)-based near infrared chromophores with two-photon absorbing properties. Tetrahedron. 66, 8629-8634.

[32] Han, Y., Kashiwazaki, G., Morinaga, H., Matsumoto, T., Hashiya, K., Bando, T., Harada, Y., and Sugiyama, H. (2013). Effect of single pyrrole replacement with b-alanine on DNA binding affinity and sequence specificity of hairpin pyrrole/imidazole polyamides targeting 50-GCGC-30. Bioorganic & Medicinal Chemistry. 21, 5436–5441.

[33] Meier, J. L., Yu, A. S., Korf, I., Segal, D. J., and Dervan, P. B. (2012). Guiding the Design of Synthetic DNA-Binding Molecules with Massively Parallel Sequencing. Journal of the American Chemical Society. 134(42), 17814–17822.

[34] Georgiev, N. I., Sakr, A. R., and Bojinov, V. B. (2011). Design and synthesis of novel fluorescence sensing perylene diimides based on photoinduced electron transfer. Dyes and Pigments. 91, 332-339.

[35] Artese, A., Costa, G., Distinto, S., Moraca, F., Ortuso, F., Parrotta, L., and Alcaro, S. (2013). Toward the design of new DNA G-quadruplex ligands through rational analysis of polymorphism and binding data. European Journal of Medicinal Chemistry. 68, 139-149.

[36] Cazacu, M., Vlad, A., Airinei, A., Nicolescu, A., and Stoica, I. (2011). New imides based on perylene and siloxane derivatives. Dyes and Pigments. 90, 106-113.

[37] Kaur, B., Quazi, N., Ivanov, I., and Bhattacharya, S. N. (2012). Near-infrared reflective properties of perylene derivatives. Dyes and Pigments. 92 , 1108-1113.

[38] Dinçalp, D., Kızılok, Ş., and Içli, S. (2010). Fluorescent macromolecular perylene diimides containing pyrene or indole units in bay positions. Dyes and Pigments. 86, 32-41.

[39] Miasojedovas, A., Kazlauskas, K., Armonaite, G., Sivamurugan, V., Valiyaveettil, S., Grazulevicius, J. V., and Jursenas, S. (2012). Concentration effects on emission of bay-substituted perylene diimide derivatives in a polymer matrix. Dyes and Pigments. 92, 1285-1291.

[40] Liang, Y., Wang, H., Wang, D., Liu, H., and Feng, S. (2012). The synthesis, morphology and liquid-crystalline property of polysiloxane-modified perylene derivative. Dyes and Pigments. 95, 260-267.

[41] Schoonover, M., and Kerwin, S. M. (2012). G-quadruplex DNA cleavage preference and identification of a perylene diimide G-quadruplex photocleavage agent using a rapid fluorescent assay. Bioorganic & Medicinal Chemistry. 20, 6904–6918.

[42] Dinçalp, H., Kızılok, Ş., Birel, Ö. H., and İçli, S. (2012). Synthesis and G-quadruplex binding study of a novel full visible absorbing perylene diimide dye. Journal of Photochemistry and Photobiology A: Chemistry. 235, 40– 48.

[43] Refiker, H., and Icil, H. (2011). Amphiphilic and Chiral Unsymmetrical Perylene Dye for Solid-State Dye-Sensitized Solar Cells. Turk J Chem. 35, 847-859.

[44] Savenije T. J. organic solar cells. Delft University of Technology.

[45] Sharma, G. D., Kurchania, R., Ball, R. J., Roy, M. S., and Mikroyannidis, J. A. (2012). Effect of Deoxycholic Acid on the Performance of Liquid Electrolyte